

# Translocation of Glycosylphosphatidylinositol-Anchored Proteins from Plasma Membrane Microdomains to Lipid Droplets in Rat Adipocytes Is Induced by Palmitate, H<sub>2</sub>O<sub>2</sub>, and the Sulfonylurea Drug Glimepiride

Günter Müller, Susanne Wied, Nicole Walz, and Christian Jung

*Sanofi-Aventis Pharma Germany, Frankfurt am Main, Germany*

Received November 28, 2007; accepted February 13, 2008

## ABSTRACT

Inhibition of lipolysis by palmitate, H<sub>2</sub>O<sub>2</sub>, and the antidiabetic sulfonylurea drug, glimepiride, in rat adipocytes has been shown previously to rely on the concerted degradation of cAMP by the glycosylphosphatidylinositol (GPI)-anchored phosphodiesterase Gce1 and 5'-nucleotidase CD73, which both gain access to the lipid droplets (LDs). The present report demonstrates the translocation of Gce1 and CD73, harboring the intact GPI anchor, from detergent-insoluble glycolipid-enriched plasma membrane domains (DIGs) to the LDs in response to palmitate, H<sub>2</sub>O<sub>2</sub>, and glimepiride by analysis of their steady-state distribution using photoaffinity labeling and activity determination as well as of their redistribution after pulse or equilibrium metabolic labeling. We were surprised to find that palmitate, H<sub>2</sub>O<sub>2</sub>, and glimepiride induced the activation of the GPI-specific phospholipase C

(GPI-PLC) at DIGs of rat adipocytes, leading to anchorless Gce1 and CD73. Inhibition of the GPI-PLC or the presence of nonhydrolyzable substrate analogs of Gce1 and CD73 interfered with the palmitate-, H<sub>2</sub>O<sub>2</sub>-, and glimepiride-induced 1) lipolytic cleavage of Gce1 and CD73, 2) translocation of their GPI-anchored versions from DIGs to LDs, 3) up-regulation of cAMP degradation, and 4) inhibition of lipolysis. These data suggest a novel insulin-independent antilipolytic mechanism in rat adipocytes, which relies on the palmitate-, H<sub>2</sub>O<sub>2</sub>-, and glimepiride-induced and GPI-PLC-dependent translocation of (c)AMP-degrading GPI-anchored proteins from the adipocyte plasma membrane to LDs. The findings may shed new light on the biogenesis and degradation of LDs in response to physiological and pharmacological stimuli.

Detergent-insoluble glycolipid-enriched membrane microdomains (DIGs), also called lipid rafts, are believed to act as platforms for the compartmentalization of various cellular processes, such as membrane transport, protein sorting, and signal transduction. They have been detected in most eukaryotic cell types on the basis of their insolubility in ice-cold, nonionic detergents, such as Triton X-100 and low buoyant density upon sucrose gradient centrifugation (Brown and Rose, 1992;

Rietveld and Simons, 1998). This characteristic of DIGs is due to the significant enrichment of cholesterol, sphingomyelin, and (glyco)sphingolipids, which are organized in the liquid-ordered state. In addition, proteins containing the stomatin/prohibitin/flotillin/HflK domain and glycosylphosphatidylinositol-anchored proteins (GPI proteins) are permanently or transiently concentrated at the cytoplasmic and exoplasmic leaflets, respectively, of the DIG plasma membrane. It is assumed that the close packing of the saturated acyl chains of the (glyco)sphingolipids and glycosylphosphatidylinositol anchors leads to the targeting of GPI proteins to DIGs (Rajendran and Simons, 2005; Hanzal-Bayer and Hancock, 2007). It is note-

Article, publication date, and citation information can be found at <http://molpharm.aspetjournals.org>.  
doi:10.1124/mol.107.043935.

**ABBREVIATIONS:** DIG, detergent-insoluble glycolipid-enriched plasma membrane domain; ADA, adenosine deaminase; AMPCP, adenosine 5'-[ $\alpha,\beta$ -methylene]di-phosphate; Br-cAMPS, Sp-8-bromo-adenosine 3',5'-cyclic monophosphorothioate; ER, endoplasmic reticulum; FA, fatty acid; 5'-FSBA, 5'-*p*-fluorosulfonylbenzoyl-adenosine; Gce1, glycosylphosphatidylinositol-anchored cAMP-binding ectoprotein; GLUT4, glucose transporter isoform 4; GO, glucose oxidase; GPI, glycosylphosphatidylinositol; GPI-PLC, glycosylphosphatidylinositol-specific phospholipase C; GPI protein, glycosylphosphatidylinositol-anchored membrane protein; hc/lcDIG, high/low cholesterol-containing detergent-insoluble glycolipid-containing membrane raft; HSL, hormone-sensitive lipase; IR, insulin receptor; LD, lipid droplet; m- $\beta$ -CD, methyl- $\beta$ -cyclodextrin; non-DIG, plasma membrane areas lacking detergent-insoluble glycolipid-enriched plasma membrane domains; 5'-Nuc, nucleotidase; PDE, phosphodiesterase; PAGE, polyacrylamide gel electrophoresis; CRD, cross-reactive determinant; TEPP, Tris-HCl/EDTA/phosphatase/protease; MES, 2-(*N*-morpholino)ethanesulfonic acid; BSA, bovine serum albumin; PLC, phospholipase C; TX-114, Triton X-114; TAG, triacylglycerol; GPI2349, *myo*-inositol-1-*O*-dodecylphosphonic acid methylester; GPI2350, *myo*-inositol-1,2-cyclo-dodecylphosphonic acid.

worthy that structural and compositional heterogeneity of DIGs has been inferred from several studies showing that different GPI proteins are located in distinct populations of DIGs in primary rat and human adipocytes (Müller et al., 2002b, 2005; Ost et al., 2005; Ortegren et al., 2006). On the basis of buoyant density and cholesterol content, at least two subclasses of DIGs have been discriminated: lcDIGs (of low cholesterol content and high buoyant density) and hcDIGs (of high cholesterol content and low buoyant density), with the GPI proteins Gce1 and CD73 being considerably enriched with hcDIGs versus lcDIGs in untreated rat adipocytes (Müller et al., 2005). Expression and targeting to DIGs of the 21- to 25-kDa cytoplasmic membrane-coat protein caveolin is believed to induce small flask-shaped invaginations in the plasma membrane, so-called caveolae, which are expressed at high levels in adipocytes (Anderson, 1998; Parton et al., 2006). Thus, both DIGs and caveolae are dynamic structures, the protein composition and function of which may change with time and in response to certain endogenous or exogenous stimuli (Müller, 2002; Parton and Richards, 2003).

Evidence has been increasing that in 3T3-L1 adipocytes and other cell lines, caveolin and stomatin, formerly regarded to be confined exclusively to caveolae/DIGs, may also reside in LDs under certain metabolic conditions (e.g., exposure to high levels of oleic acid) (Fujimoto et al., 2001; Umlauf et al., 2004; Martin and Parton, 2005; Robenek et al., 2005). Most recently, certain GPI protein family members, which hitherto are believed to reside exclusively at plasma membrane DIGs in mammalian cells, have been found to be associated with LDs of rat adipocytes under certain metabolic conditions. The GPI-anchored cAMP-binding ectoprotein and phosphodiesterase (PDE) Gce1, as well as AMP-binding ectoprotein and 5'-nucleotidase (5'-Nuc), CD73, have been recovered with LDs of rat adipocytes in response to lipolysis inhibition by palmitate,  $H_2O_2$ , and glimepiride (Müller et al., 2008a). In contrast, in the basal state, both Gce1 and CD73 behave as typical cell surface ectoproteins (Klip et al., 1988; Müller et al., 1993, 1994a). Moreover, purified Gce1 harboring the intact GPI anchor was shown to interact with isolated adipocyte LDs and to exchange between distinct LDs in vitro, which strongly suggested that a subset of GPI proteins can act as resident LD-associated proteins. Together, these findings raised the possibility that in adipocytes, DIGs and LDs operate as dynamic organelles redistributing subsets of their typical constituent proteins, such as caveolin and certain GPI proteins, rather than represent static structures.

In the present study, the translocation of Gce1 and CD73 in response to physiological conditions (high levels of FAs and  $H_2O_2$ ) or pharmacological stimuli (glimepiride) from plasma membrane DIGs to LDs was demonstrated in primary rat adipocytes using several biochemical approaches, and its role in metabolic signaling was investigated. The findings may have implications for our current understanding of GPI protein function and trafficking and LD biogenesis and lipolysis regulation.

## Materials and Methods

**Materials.** [ $^3H$ ]cAMP was purchased from Amersham-Buchler (Braunschweig, Germany). GPI2350, GPI2349, and  $\beta$ -amidotaurocholate were made available by the pharma synthesis department of Sanofi-Aventis Pharma (Frankfurt, Germany); wortmannin, Triac-

sin C, brefeldin A, and anti-glucose transport isoform-4 (GLUT4) antibodies were delivered by Calbiochem (Bad Soden, Germany), cAMP, AMP, Sp-8-bromo-adenosine 3'-5'-cyclic monophosphorothioate (Br-cAMPS), adenosine 5'-[ $\alpha,\beta$ -methylene]diphosphate (AMPCP), 5'-Nuc (*Crotalus atrox*), and PDE (bovine brain) were bought from Sigma (Deisenhofen, Germany); cholesterol oxidase and "complete" protease inhibitor mix were obtained from Roche Molecular Biochemicals (Mannheim, Germany); anti-IR antibodies were delivered by Millipore (Billerica, MA); anti- $\alpha$ -flotillin-1 (reggie-2) monoclonal antibodies were purchased from BD Biosciences (San Jose, CA); recombinant GPI-PLC (*Trypanosoma brucei*) and anti-cross-reactive determinant (CRD) antibodies were obtained from Oxford Glycosystems (Oxford, UK); anti-caveolin-1 (rabbit) and anti-pp59<sup>Lyn</sup> (clone 32) antibodies were purchased from Transduction Laboratories (Lexington, KY). The sources for all other materials were described previously (Müller et al., 1993, 1994b, 2001, 2002a, 2005, 2008a,b).

**Metabolic Labeling of Rat Adipocytes with [ $^{14}C$ ]Inositol.** The incubation was performed as described previously (Müller et al., 2008b) but for 5 min for short-term pulse labeling or 60 min for long-term equilibrium labeling in the presence of the various agents and/or inhibitors as indicated. For initiation of the chase, the cells were washed twice by flotation with 10 ml each of labeling medium containing 0.5 mM glucose and 10 mM *myo*-inositol and then suspended in 20 ml of the same medium (0 time point). After incubation (37°C, gentle shaking) for increasing periods of time in the presence of various agents and/or inhibitors as indicated, the adipocytes were separated from the medium by flotation and washed with labeling medium (15°C).

**Preparation of Microsomes, Plasma Membranes, hc/lcDIGs, and non-DIGs.** For the preparation of plasma membranes, washed rat adipocytes ( $3.5 \times 10^8$  cells) were homogenized in 10 ml of lysis buffer (25 mM Tris-HCl, pH 7.4, 0.5 mM EDTA, 0.25 mM EGTA, 0.25 M sucrose, 50 mM NaF, 5 mM sodium pyrophosphate, 25 mM glycerol-3-phosphate, 10  $\mu$ M okadaic acid, and 1 mM sodium orthovanadate containing "complete" protease inhibitor mix) using a motor-driven Teflon-in-glass homogenizer (10 strokes with a loose-fitting pestle) at 22°C (Müller et al., 1994c). The defatted infranant obtained after centrifugation (1500g, 5 min) was centrifuged (12,000g, 15 min). Microsomes were collected from the supernatant by centrifugation (100,000g, 1 h) and then suspended in TEPP buffer [10 mM Tris-HCl, pH 7.4, 2 mM EDTA containing phosphatase (50 mM NaF, 5 mM sodium pyrophosphate, 10  $\mu$ M okadaic acid, 1 mM sodium orthovanadate) and protease inhibitor mixes; see above] at 2 to 3 mg of protein/ml. The pellet of the 12,000g spin was suspended in 10 ml of lysis buffer layered on top of a 5-ml cushion of 38% (w/v) sucrose, 25 mM Tris/HCl, pH 7.4, and 1 mM EDTA and then centrifuged (110,000g, 1 h). Total plasma membranes were removed at the interface between the two layers by suction (0.5 ml) after 5-fold dilution collected by centrifugation (45,000g, 30 min) and finally resuspended in TEPP buffer at 0.5 to 1 mg protein/ml.

For preparation of DIGs, the pelleted plasma membranes (200–400  $\mu$ g of protein) were suspended in 800  $\mu$ l of 25 mM MES/KOH, pH 6.0, 1% Triton X-100, 150 mM NaCl, 35% sucrose, 5 mM EDTA, 20 mM NaF, and protease inhibitor mix by 10 strokes with a pistil fitting to 1.5-ml microcentrifuge tubes and then incubated (1 h, on ice). Two 200- $\mu$ l cushions of the same medium containing 22 and 5% sucrose, respectively, were laid over in sequential fashion. After centrifugation (26,000g, 30 min, 4°C, tabletop rotor; Beckman Coulter, Fullerton, CA), the light-scattering opalescent bands of flocculent material at the 5 to 22% and 22 to 35% sucrose interfaces were collected as hcDIGs and lcDIGs, respectively, using a 19-gauge needle and a syringe (~200  $\mu$ l per fraction) and then diluted with 800  $\mu$ l of 25 mM MES/KOH, pH 6.0, 150 mM NaCl, 5 mM EDTA, and 20 mM NaF and protease inhibitor mix and finally centrifuged (48,000g, 15 min, 4°C). Density of the fractions was determined by measuring the refractive index. For preparation of plasma membrane areas lacking DIGs (non-DIGs), the Triton X-100-soluble proteins from the layer below the 35% sucrose interface (~600  $\mu$ l) were removed and

then precipitated under native conditions. The collected DIGs and non-DIGs were suspended in TEPP buffer at 0.1 to 0.5 mg of protein/ml. hcDIGs, lcDIGs, and non-DIGs were characterized by the determination of relevant markers as described previously (Müller et al., 2002b, 2005) with typical enrichment (hc/lcDIGs) and deprivation (non-DIGs) of caveolin-1 (8.5- to 11.6-fold/3.7- to 7.5-fold, and 0.3- to 0.6-fold), caveolin-2 (5.2- to 6.5-fold/3.1- to 4.7-fold, and 0.1- to 0.2-fold), and cholesterol (3.0- to 3.5-fold corresponding to  $0.81 \pm 0.12$  nmol/ $\mu$ g protein/1.9- to 2.5-fold corresponding to  $0.55 \pm 0.10$  nmol/ $\mu$ g protein, and 0.5- to 0.8-fold corresponding to  $0.13 \pm 0.05$  nmol/ $\mu$ g protein) compared with total plasma membranes.

**Protein Extraction from DIGs.** DIGs in 50 mM HEPES/KOH, pH 7.4, 150 mM NaCl, 1% Triton X-100, 5 mM  $\text{MgCl}_2$ , 0.1 mM EDTA, and protease inhibitor mix (0.1–0.3 mg protein/ml) were incubated (1 h, 4°C, several cycles of vortexing) with 60 mM octyl glucoside and 0.4%  $\beta$ -amidotauricholate (Müller et al., 1994b). After centrifugation (100,000g, 30 min, 4°C), the supernatant proteins were used for precipitation under native conditions.

**TAG Synthesis by DIGs.** DIGs (100–150  $\mu$ g of protein) were incubated with 200  $\mu$ M [ $^3\text{H}$ ]glycerol-3-phosphate (5  $\mu$ Ci) in 500  $\mu$ l of LD buffer (500  $\mu$ M oleoyl-CoA, 100  $\mu$ M oleic acid, 200  $\mu$ M CoA, 2 mM ADP, 10 mM creatine phosphate, 0.2 U/ml creatine kinase, 50 mM Tris/HCl, pH 7.4, 10 mM  $\text{MgCl}_2$ , 0.5 mM dithiothreitol, 140 mM KCl, 250 mM sucrose, and 0.5% BSA). After brief sonication (bath sonifier) and incubation (30 min, 37°C), the reactions were terminated by the addition of 5 ml of toluene-based scintillation cocktail (Quickscint 501; Zinsser, Frankfurt, Germany). After incubation (12 h, 25°C), the radioactivity recovered in the organic phase was determined by liquid scintillation counting. Blank values of incubations lacking protein were subtracted in each case to correct for unspecific partitioning of [ $^3\text{H}$ ]glycerol-3-phosphate.

**LD Formation by DIGs.** DIGs (200–250  $\mu$ g of protein) were incubated (1 h, 37°C) with cytosol prepared from basal rat adipocytes (100–150  $\mu$ g of protein) in 0.75 ml of LD buffer containing protease inhibitor mix as described for the measurement of TAG synthesis. Thereafter, the samples were adjusted to 40% sucrose, and 1.5-ml samples were sequentially overlaid with 3 ml of 50 mM Tris-HCl, pH 7.5, 25% sucrose, 10 mM EDTA, and finally with 1 ml of 50 mM Tris-HCl, pH 7.5, 10 mM EDTA. After centrifugation (160,000g, 18 h, 4°C; SW55Ti rotor, Beckman Coulter), the gradient was divided into five fractions with mean densities (grams per milliliter) of 1.051 (1.5 ml), 1.092 (1 ml), 1.118 (1 ml), 1.149 (1 ml), and 1.192 (1 ml).

**Determination of Enzyme Activities.** PDE activity was assayed as described previously (Hansen et al., 1982) with modifications. In brief, precipitated protein samples (10–20  $\mu$ g of protein) were dissolved in 300  $\mu$ l of 50 mM HEPES/KOH, pH 7.4, 0.1 mM EGTA, 8 mM  $\text{MgCl}_2$ , and 0.1 mg/ml BSA and then incubated (10 min, 30°C) with [ $^3\text{H}$ ]cAMP (10 nCi, 0.1  $\mu$ M) in the absence or presence of 3-isobutyl-1-methylxanthine (100  $\mu$ M) or isoform-specific inhibitors as indicated. Under these conditions, no more than 20% of the substrate was hydrolyzed. 5'-Nuc (*Crotalus atrox* venom, 0.5 mU) was added, and the incubation continued (30 min, 30°C) for complete dephosphorylation of 5'-AMP to adenosine. Adenosine was separated from residual cAMP by passage over diethylaminoethanol-Sephadex A-25 columns and then determined by liquid scintillation counting. The activity of the different PDE isoforms was calculated as the difference between the absence and presence of a specific inhibitor (0.5  $\mu$ M cilostamide for PDE3, 5  $\mu$ M rolipram for PDE4). PDE activities were proportional to time and the protein amount used. 5'-Nuc was assayed as described previously (Avruch and Wallach, 1971) with modifications (Müller et al., 1993). In brief, precipitated protein samples (20–50  $\mu$ g of protein) were dissolved in 100  $\mu$ l of 100 mM Tris-HCl, pH 7.4, and 20 mM  $\text{MgCl}_2$  and then incubated (30 min, 37°C) with [ $^3\text{H}$ ]AMP (150 nCi, 100  $\mu$ M). After termination of the reaction by the addition of  $\text{ZnSO}_4$  (250 mM, final concentration), unhydrolyzed AMP was removed by precipitation with 250  $\mu$ l of 0.3 M  $\text{Ba}(\text{OH})_2$  and subsequent centrifugation (10,000g, 2 min). The supernatant was determined for radiolabeled

adenosine by liquid scintillation counting (5 ml of Zinsser cocktail 361).

**Miscellaneous.** Published procedures were used for the preparation (Müller et al., 2003) and incubation of rat adipocytes with insulin, glimepiride, glucose oxidase (GO), and palmitate bound to BSA (Müller et al., 2008b), preparation of LDs and cytosol (Müller et al., 2008a,b), preparation of methyl- $\beta$ -cyclodextrin (m- $\beta$ -CD)-cholesterol inclusion complexes and cholesterol depletion of adipocytes (Müller et al., 2002b), photoaffinity labeling with 8- $\text{N}_3$ -[ $^{32}\text{P}$ ]cAMP (Müller et al., 1994a) or [ $^{14}\text{C}$ ]5'- $p$ -fluorosulfonylbenzoyl adenosine (5'-FSBA; Stochaj and Mannherz, 1990), protein extraction from LDs and protein precipitation, affinity purification of Gce1 and CD73 by adsorption to cAMP/AMP-Sepharose, determination of cAMP-to-adenosine conversion, and determination of cholesterol using cholesterol oxidase (Müller et al., 2008a,b), incubation with phosphatidylinositol-specific phospholipase C (PLC) (Müller et al., 1994a), TX-114 partitioning (Bordier, 1981), determination of lipolysis by measurement of glycerol and FA release (Müller et al., 2003), determination of hormone-sensitive lipase (HSL) translocation (Müller et al., 2008b), Phosphor Imaging was performed with a Phosphor Imager (GE Healthcare, Chalfont St. Giles, Buckinghamshire, UK), chemiluminescent imaging with a Lumi Imager (Roche Diagnostics, Mannheim, Germany), SDS-polyacrylamide gel electrophoresis (PAGE; 4 to 12% Bis-Tris precast gel, pH 6.4, MES/SDS running buffer) under reducing conditions, immunoblotting using chemiluminescent detection (Müller et al., 2001), determination of protein using the BCA method (Pierce, Rockford, IL) with BSA as calibration standard, calculation of  $\text{EC}_{50}$  values, and construction of figures from PhosphorImages + Lumi Images (Müller et al., 2005). Differences between the experimental groups were determined using analysis of variance with statistical significance set at  $P$  values of  $<0.05$ .

## Results

**Effect of Insulin, Palmitate, Glimepiride, and  $\text{H}_2\text{O}_2$  on the Intracellular Distribution of Gce1 and CD73 in Rat Adipocytes.** The GPI proteins Gce1 and CD73 had been localized at DIGs of the plasma membrane of adipocytes (Klip et al., 1988; Müller et al., 1993, 1994a,c). However, then they were identified also at LDs acting as a cAMP-degrading PDE (Gce1) and AMP-degrading 5'-Nuc (CD73) on the basis of a variety of biochemical evidences, such as photoaffinity and metabolic labeling, affinity purification and depletion, immunoreactivity and enzymatic activity, and inhibition of their activities upon interference with their LD expression (Müller et al., 2008a). Therefore, the possibility was studied that DIGs operate as storage compartments for Gce1 and CD73 for their delivery to LDs during inhibition of lipolysis by treatment of isolated rat adipocytes with palmitate, glimepiride, and GO (for the generation of  $\text{H}_2\text{O}_2$ ), as has been reported previously (Müller et al., 2008b). The isoproterenol-, adenosine deaminase-, and forskolin-induced release of glycerol and FAs into the incubation medium of adipocytes is known to be reduced with varying maximal potencies and  $\text{IC}_{50}$  values by insulin (80–90%, 0.05–0.08 nM), palmitate (45–55%, 0.4–0.5 mM), glimepiride (55–65%, 0.8–1.4  $\mu$ M), and GO (70–80%, 2–4 mU/ml) (Müller et al., 2008b).

To obtain a first hint for involvement of DIGs, they were disrupted by cholesterol depletion using m- $\beta$ -CD under conditions, which do not affect cell viability (Müller et al., 2002b), before treatment of the adipocytes with palmitate, glimepiride, and GO. Thereafter, LDs were prepared and assayed for the expression of Gce1 and CD73 by the determination of the conversion of cAMP to adenosine through their concerted PDE (Gce1) and 5'-Nuc (CD73) activities (Table 1). The glimepiride-,

palmitate-, and GO-induced cAMP-to-adenosine conversion was diminished by 60 to 85% with LDs from cholesterol-depleted adipocytes compared with untreated cells. The isoproterenol-induced lipolysis measured in parallel was found to be reduced in untreated adipocytes by 50 to 70% in response to glimepiride, palmitate, and GO compared with control cells but to resist significant suppression in cholesterol-depleted cells. Treatment of the adipocytes with stoichiometric amounts of m- $\beta$ -CD and m- $\beta$ -CD-cholesterol inclusion complexes, which does not lead to net transfer of cholesterol to or from DIGs (Müller et al., 2002b), failed to significantly compromise the up-regulated cAMP-to-adenosine conversion and the inhibited lipolysis (Table 1). These findings strongly suggest that the observed effects are caused by the specific disruption of DIGs in the course of cholesterol depletion rather than by the presence of m- $\beta$ -CD, per se. Taken together, the abrogation of the palmitate-, glimepiride-, and H<sub>2</sub>O<sub>2</sub>-induced up-regulation of the PDE and 5'-Nuc activities at LDs as well as lipolysis inhibition in adipocytes lacking DIGs provided first evidence for a role of these structures as source or storage site for the GPI proteins Gce1 and CD73 before their translocation to the LDs.

For direct demonstration of the regulated translocation of Gce1 and CD73 from hcDIGs to LDs, these structures were prepared from palmitate-, glimepiride-, and GO-treated rat adipocytes and then subjected to photoaffinity labeling of Gce1 with 8-N<sub>3</sub>-[<sup>32</sup>P]cAMP and CD73 with [<sup>14</sup>C]5'-FSBA. Control experiments on basis of quantitative [<sup>3</sup>H]cAMP- and [<sup>3</sup>H]AMP-binding filtration assays and an assumed binding stoichiometry of one nucleotide per protein molecule had revealed that photoaffinity labeling of both proteins is not quantitative with different efficacies for isolated DIGs (Gce1, 0.7–1.5%; CD73, 2.5–3.5%) and LDs (Gce1, 5–8%; CD73, 9–13%). But it is important to note that the efficacies had turned out to be of low variance between different labelings of the same DIGs or LD preparations (less than 10%) or labelings of different preparations from the same cells (less than 20%) and to be linear within the range of total amounts of DIGs and LD protein routinely used. Thus, photoaffinity labeling of isolated DIGs and LDs can be used to reliably follow the relative distribution and translocation of Gce1 and CD73 between these compartments.

The phosphorimages of the SDS-PAGE for the above experiment revealed significant concentration-dependent decreases in the amount of photoaffinity-labeled Gce1 and CD73 recovered with hcDIGs (Fig. 1A) in response to palmitate (by 72 and 59%, respectively, at 2 mM), glimepiride (by 77 and 56%, respectively, at 20  $\mu$ M) and GO (by 82 and 69%,

respectively, at 100 mU/ml). These decreases were paralleled by the palmitate-/glimepiride-/GO-induced increases in the amounts of LD-associated Gce1 (by 224/281/384%) and CD73 (98/169/329%)(Fig. 1B). The specificity of the photoaffinity labeling reactions was demonstrated by the almost complete quenching of labeling of Gce1 and CD73 by excess of cAMP and AMP, respectively. For a given stimulus, the incremental increases at LDs and decreases at hcDIGs of the Gce1 and CD73 protein amounts and of the PDE and 5'-Nuc activities, and the corresponding EC<sub>50</sub> values were very well correlated (Fig. 1C). These data indicated that palmitate, glimepiride, and GO action modify the steady-state distribution of Gce1 and CD73 between hcDIGs and LDs of rat adipocytes leading to their enrichment at LDs and deprivation at hcDIGs.

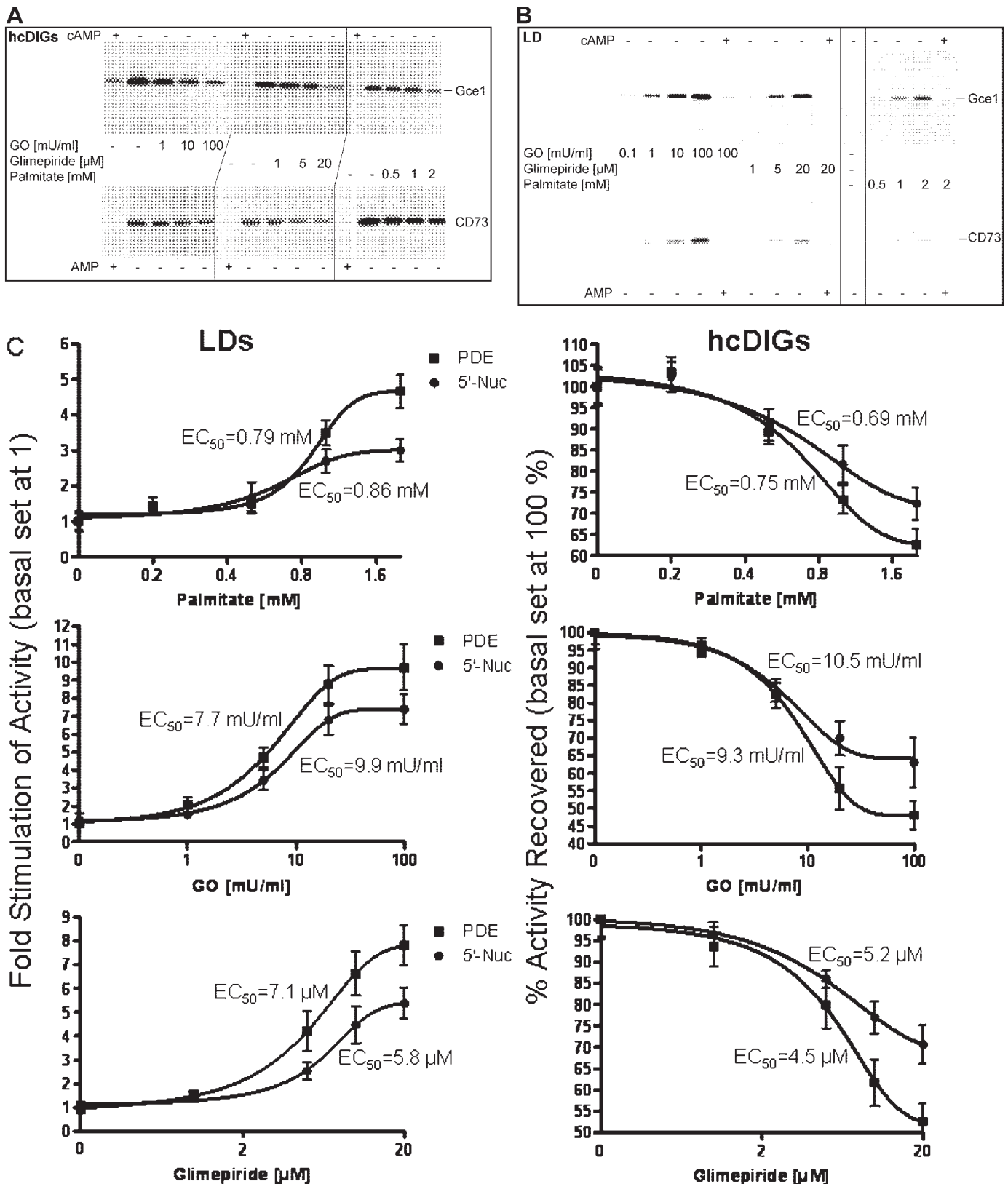
To follow the translocation process of Gce1 and CD73 from hcDIGs to LDs, pulse-chase experiments were performed with stimulated adipocytes after metabolic labeling of their GPI anchors with [<sup>14</sup>C]inositol. The retention of the inositol residue within the phosphoinositol glycan moiety of the GPI anchor of both intact and lipolytically cleaved GPI proteins in combination with the low metabolism of inositol into other carbohydrates in rat adipocytes during the pulse-chase periods used has been demonstrated in previous studies (Müller et al., 1993) and enables monitoring of the intracellular trafficking of GPI proteins in general. After incubation of rat adipocytes with [<sup>14</sup>C]inositol for 5 min (pulse labeling; Fig. 2, A and C) or 60 min (equilibrium labeling; Fig. 2, B and C) followed by the addition of excess of unlabeled *myo*-inositol in the presence of palmitate, GO or glimepiride for increasing periods of time, Gce1 and CD73 were affinity-purified from the isolated hcDIGs and LDs by adsorption to cAMP- and AMP-Sepharose, respectively, and then analyzed by SDS-PAGE. Phosphorimaging (Fig. 2A) and quantitative evaluation (Fig. 2C) revealed that in pulse-labeled basal adipocytes the amounts of [<sup>14</sup>C]inositol-labeled Gce1 and CD73 at hcDIGs increased during the initial 10 to 60 min of chase and subsequently declined until the end of the chase. In the presence of palmitate, GO and glimepiride during the chase period the peak and final levels of Gce1 and CD73 at hcDIGs were significantly lower than in the basal state. In contrast, the continuous increases in [<sup>14</sup>C]inositol-labeled Gce1 and CD73 at LDs observed to up to 120 min of chase were significantly higher with stimulated than basal adipocytes (Fig. 2, A and C). In adipocytes labeled at equilibrium, the amounts of [<sup>14</sup>C]inositol-labeled Gce1 and CD73 at hcDIGs decreased continuously during the chase period and more rapidly in the presence of palmitate, GO and glimepiride (15–60 min half-

TABLE 1

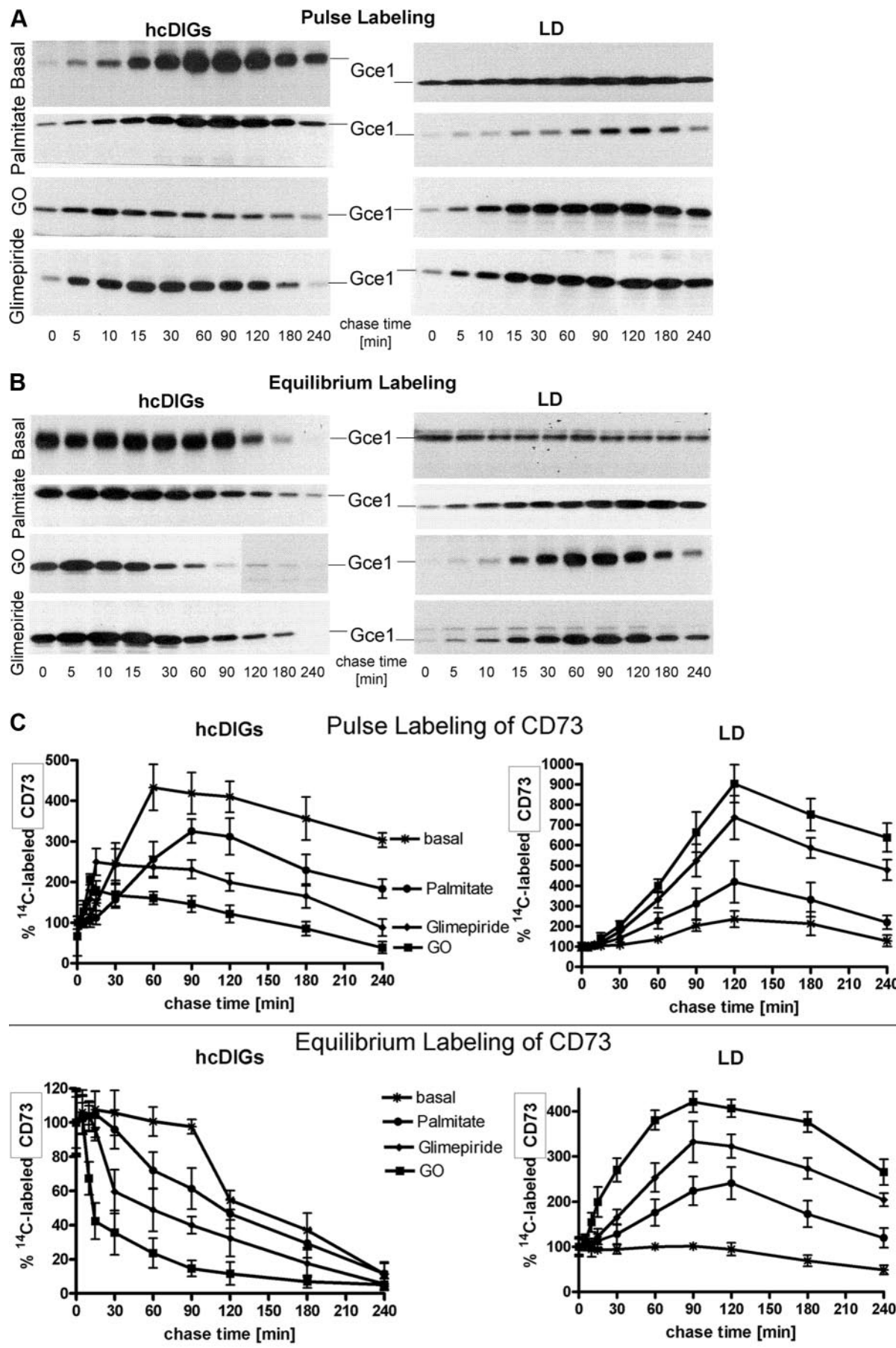
Effect of cholesterol depletion on the cAMP-to-adenosine conversion by LDs and lipolysis

Isolated rat adipocytes were incubated (50 min, 37°C) in the absence or presence of 3.8 mM m- $\beta$ -CD or 1.9 mM m- $\beta$ -CD plus 1.9 mM m- $\beta$ -CD-cholesterol complex. Thereafter, the cells were incubated (37°C) with palmitate (1 mM, 120 min), glimepiride (10  $\mu$ M, 60 min), GO (10 mU/ml, 20 min), or buffer alone (control). Portions of the adipocytes were separated from the medium for the preparation of LDs, which were then assayed for cAMP-to-adenosine conversion. Other portions of the adipocytes were incubated with isoproterenol (1  $\mu$ M, 2 h, 37°C) and then separated from the medium for the analysis of the glycerol released. cAMP-to-adenosine conversion by LDs prepared from untreated adipocytes was set at 100% for each antilipolytic challenge. Isoproterenol-induced lipolysis of control adipocytes was set at 100% (means  $\pm$  S.D., *n* = 3 independent adipocyte preparations/incubations). Bold numbers indicate significant difference (*P* < 0.05) compared with the untreated and correspondingly glimepiride-, palmitate-, and GO-challenged adipocytes.

Treatment	cAMP-to-Adenosine Conversion			Isoproterenol-Induced Lipolysis			
	Glimepiride	Palmitate	GO	Control	Glimepiride	Palmitate	GO
	%			%			
m- $\beta$ -CD	100 $\pm$ 17	100 $\pm$ 12	100 $\pm$ 14	100 $\pm$ 6	39 $\pm$ 4	51 $\pm$ 3	29 $\pm$ 2
m- $\beta$ -CD + cholesterol	<b>28 <math>\pm</math> 5</b>	<b>20 <math>\pm</math> 3</b>	<b>35 <math>\pm</math> 6</b>	<b>87 <math>\pm</math> 3</b>	<b>90 <math>\pm</math> 4</b>	<b>89 <math>\pm</math> 3</b>	<b>90 <math>\pm</math> 5</b>
	85 $\pm$ 9	92 $\pm$ 10	105 $\pm$ 17	91 $\pm$ 5	36 $\pm$ 2	45 $\pm$ 3	26 $\pm$ 3



**Fig. 1.** Effect of palmitate, glimepiride, and GO action on the steady-state distribution of Gce1 and CD73 proteins as well as PDE and 5'-Nuc activities between hcDIGs and LDs. Isolated rat adipocytes were incubated (60 min, 37°C) in the absence (basal) or presence of increasing concentrations of palmitate, glimepiride, or GO as indicated and then used for the preparation of hcDIGs and LDs. Proteins were extracted from the hcDIGs (A and C) and LDs (B and C) and then precipitated under native conditions. Portions of the solubilized proteins were photoaffinity-labeled with  $N_3$ -[ $^{32}$ P]cAMP or [ $^{14}$ C]5'-FBSA in the absence or presence of unlabeled 10 mM cAMP or AMP for the detection of Gce1 or CD73, respectively, and then precipitated under denaturing conditions and after solubilization were separated by SDS-PAGE. The phosphorimages of a typical experiment are shown repeated two times with similar results. Other portions of the solubilized proteins were assayed for PDE and 5'-Nuc activities (C). Quantitative evaluations (means  $\pm$  S.D.,  $n = 4$  independent adipocyte preparations and activity determinations) are given. The activities recovered with LDs and hcDIGs are set at 1 (fold stimulation) and 100% (activity recovered), respectively, for each treatment.



life times) compared with basal cells (90–120 min). In contrast, the amounts of [ $^{14}\text{C}$ ]inositol-labeled Gce1 and CD73 at LDs increased in the presence of palmitate, GO, and glimepiride during the chase to up to 90 to 120 min and thereafter declined until the end of the chase (Fig. 2, B and C). In basal adipocytes [ $^{14}\text{C}$ ]inositol-labeled Gce1 and CD73 at LDs remained constant until 120 min and then slightly declined. Taken together, the (lower) increases during pulse labeling and the (more rapid) losses during equilibrium labeling of Gce1 and CD73 at hcDIGs in (stimulated versus basal) adipocytes were accompanied by (more pronounced) increases of Gce1 and CD73 at LDs in (stimulated versus basal) adipocytes during both pulse and equilibrium labelings. These relationships are compatible with the translocation of Gce1 and CD73 from hcDIGs to LDs in rat adipocytes, which is significantly up-regulated in response to palmitate, glimepiride, and GO action. The rankings of the potencies for translocation, cAMP-to-adenosine conversion by LDs, and inhibition of lipolysis are identical (GO > glimepiride > palmitate).

Recent investigations showed that Gce1 and CD73 are apparently redistributed from hcDIGs to lcDIGs upon challenge of adipocytes with glimepiride (Müller et al., 2001). To test whether Gce1 and CD73 move via lcDIGs during their translocation from hcDIGs to LDs, hcDIGs, lcDIGs, and LDs were prepared from palmitate-, glimepiride-, and GO-treated rat adipocytes and subsequently analyzed for the presence of Gce1 and CD73 by photoaffinity labeling, the typical DIG-associated proteins caveolin-1 and flotillin-1 (reggie-2) and the typical LD-associated proteins HSL and perilipin-A by immunoblotting, cholesterol by enzymatic measurement and TAG-synthesizing enzymes by determination of TAG synthesis as glycerol-3-phosphate incorporation into TAG (Fig. 3). As expected, in the basal state, Gce1 and CD73 (Fig. 3A) and cholesterol (Fig. 3D) were significantly enriched at hcDIGs versus lcDIGs, whereas the opposite was true for perilipin-A (Fig. 3B), flotillin-1 (Fig. 3C), and TAG-synthesizing enzymes (Fig. 3D). Caveolin-1 was distributed approximately equally between hcDIGs and lcDIGs (Fig. 3C). LDs harbored the highest amounts of HSL, perilipin-A, flotillin-1, and cholesterol but only low levels of Gce1, CD73, caveolin-1, and TAG-synthesizing enzymes (Fig. 3, C and D). Microsomes contained minute amounts of perilipin-A and HSL (data not shown), caveolin-1, and flotillin-1 (Fig. 3C), which is in agreement with its identification in endosomes and the trans-Golgi network in adipocytes (Langhorst et al., 2005). A trend for elevated amounts of perilipin-A, caveolin-1, and flotillin-1 at lcDIGs upon challenge with palmitate, glimepiride, and GO was observed, however, that did not result in detectable changes in the abundance of perilipin-A and caveolin-1 at hcDIGs and LDs and of the relative distribution of flotillin-1 as well as cholesterol and TAG-synthesizing enzymes between hcDIGs, lcDIGs, and LDs (Fig. 3, B–D). This demon-

strated maintenance of the subcompartmentalization of the adipocyte plasma membrane and of the structure of LDs in adipocytes in the course of suppressed lipolysis. It is noteworthy that all three stimuli (GO > glimepiride > palmitate) induced slight but significant increases in the amounts of Gce1 and CD73 at lcDIGs, which were paralleled by pronounced increases at LDs and decreases at hcDIGs (Fig. 3A). These relationships are compatible with the translocation of the GPI proteins from hcDIGs to LDs via lcDIGs. Thus, in contrast to the storage compartment hcDIGs, lcDIGs may act as an intermediary or transient compartment for GPI proteins, which would corroborate the previously recognized heterogeneity of DIGs at rat adipocyte plasma membranes on the basis of differences in their protein composition (see Introduction). However, direct and simultaneous translocation of GPI proteins from hcDIGs to LDs and lcDIGs cannot be excluded at present.

The specificity of the translocation of Gce1 and CD73 from hcDIGs to LDs in rat adipocytes was addressed by immunoblotting for the typical marker proteins: caveolin-1 as structural protein anchored at the inner leaflet of plasma membrane caveolae, p59<sup>Lyn</sup> as the dually acylated nonreceptor tyrosine kinase anchored at the inner leaflet of plasma membrane hcDIGs (Müller et al., 2001), GLUT4 and IR as transmembrane proteins of plasma membrane non-DIGs, and HSL and perilipin-A as LD-associated proteins. The chemiluminescent images (Fig. 4) revealed that the stimulation of lipolysis by isoproterenol and adenosine deaminase (ADA), which leads to the translocation of HSL to and perilipin-A from LDs (Müller et al., 2003; Londos et al., 2005), as well as the inhibition of the isoproterenol/ADA-induced lipolysis by palmitate, glimepiride, or GO, which blocks HSL and perilipin-A translocation, did not significantly affect the relative distribution of perilipin-A, HSL, caveolin-1, and IR between the hcDIGs and LDs. In agreement with previous studies (Müller et al., 2005), glimepiride and to a lesser degree palmitate decreased and increased the amounts of p59<sup>Lyn</sup> and GLUT4, respectively, at hcDIGs (but not LDs) compared with control and GO treatment, which is believed to mediate the IR-independent insulin-mimetic signaling of glimepiride via activated p59<sup>Lyn</sup> to glucose transport in rat adipocytes. Taken together, these findings argue for the specificity of the palmitate-, glimepiride-, and GO-induced translocation of Gce1 and CD73 from hcDIGs to LDs.

To gain first insights into the molecular mechanism underlying the stimulus-dependent translocation of GPI proteins to LDs, rat adipocytes with defective DIGs/caveolae, TAG synthesis, or vesicular trafficking were prepared by treatment with m- $\beta$ -CD for depletion of plasma membrane cholesterol, Triacsin C for inhibition of fatty acyl-CoA synthase, or brefeldin A for blockade of the ER-to-Golgi transport and then challenged with palmitate, glimepiride, or GO. Phosphorimaging of the photoaffinity-labeled Gce1 recovered with

**Fig. 2.** Effect of palmitate, glimepiride, and GO action on the translocation of Gce1 and CD73 from hcDIGs to LDs. Isolated rat adipocytes were metabolically labeled with [ $m\text{-}^{14}\text{C}$ ]inositol for 5 min (pulse labeling, A) or 60 min (equilibrium labeling, B) in the presence of isoproterenol (1  $\mu\text{M}$ ). After the addition of excess of unlabeled  $m\text{-}$ inositol (0 time points), the incubation was continued for increasing periods of time (chase) in the absence (basal) or presence of palmitate (1 mM), glimepiride (10  $\mu\text{M}$ ), or GO (100 mU/ml). hcDIGs and LDs were prepared from the washed adipocytes and then used for extraction and precipitation of the proteins under native conditions. The dissolved protein samples were analyzed for the presence of Gce1 and CD73 by affinity purification and subsequent SDS-PAGE analysis of the eluted and precipitated (under denaturing conditions) proteins. The phosphorimages of a typical experiment are shown (for Gce1 only, A and B). Quantitative evaluations (means  $\pm$  S.D.,  $n = 3$  adipocyte preparations and metabolic labelings) are given (for CD73 only, C). The amounts of  $^{14}\text{C}$ -labeled CD73 recovered with LDs and hcDIGs from basal adipocytes at the 0 time points are set at 100%.

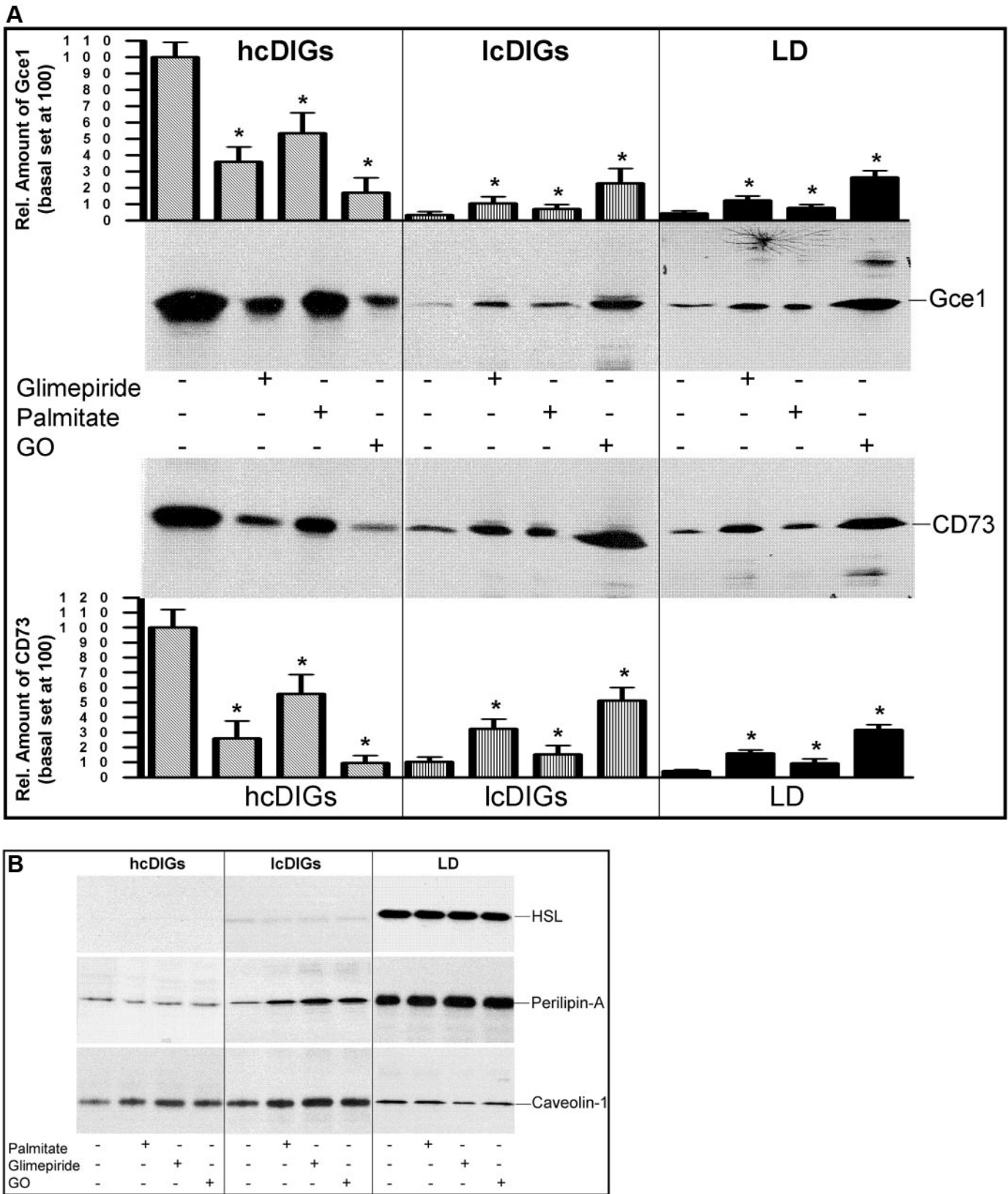
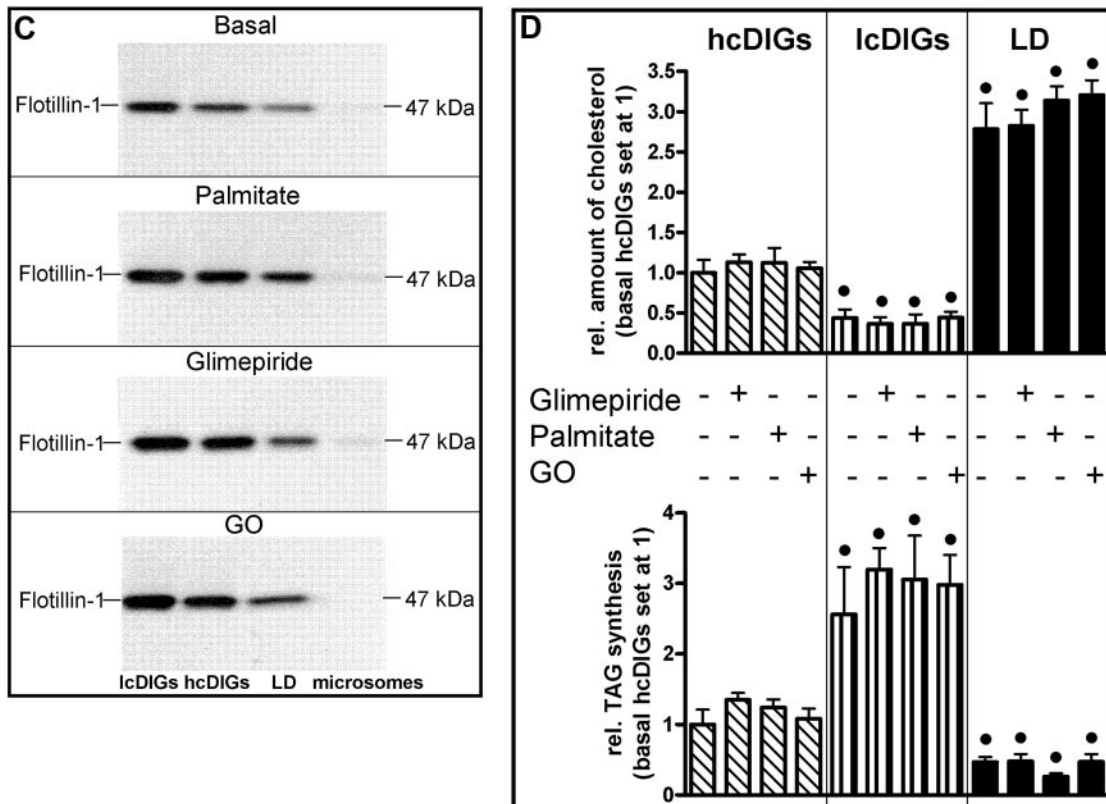


**Fig. 3.** Effect of palmitate, glimepiride, and GO action on the steady-state distribution of Gce1, CD73, HSL, caveolin, and perilipin between hcDIGs, lcDIGs, and LDs. Isolated rat adipocytes were incubated (60 min, 37°C) in the absence (basal) or presence of palmitate (1 mM), glimepiride (10  $\mu$ M), or GO (100 mU/ml) and then used for the preparation of microsomes, hcDIGs, lcDIGs, and LDs. A, from portions, proteins were extracted and precipitated under native conditions and after solubilization were photoaffinity-labeled with  $N_3$ -[ $^{32}$ P]cAMP or [ $^{14}$ C]5'-FSBA for the detection of Gce1 and CD73, respectively. The proteins were precipitated under denaturing conditions and then analyzed by SDS-PAGE. Quantitative evaluations of the phosphorimages (means  $\pm$  S.D.,  $n = 3$  independent experiments, amounts of Gce1 and CD73 at hcDIGs in the basal state set at 100) are shown. B and C, from other portions of the hcDIGs, lcDIGs, LDs, and microsomes (as indicated), proteins were extracted and precipitated under denaturing

the LDs revealed that m- $\beta$ -CD but not brefeldin A significantly diminished the challenge-dependent amounts of LD-associated Gce1 (Fig. 5). It is remarkable that Triacsin C significantly reduced the up-regulation of Gce1 at LDs in palmitate-/GO- but not glimepiride-treated adipocytes. This suggests that translocation of GPI proteins from hcDIGs to LDs does not depend on vesicular trafficking but requires intact DIGs/caveolae irrespective of the antilipolytic agent used. The differential and critical role of fatty acyl-CoA synthase may rely on the production of TAG for LD biogenesis, which could depend on the acylation of either activated free FAs in palmitate-/GO-treated adipocytes or de novo synthesized FAs in glimepiride-treated adipocytes. Previous studies demonstrated stimulation of de novo FA synthesis by glimepiride in adipocytes (Müller et al., 2005).

For a more detailed understanding of the translocation reaction, a cell-free system was introduced for the formation of LDs by hcDIGs in vitro and the concomitant translocation of GPI proteins from hcDIGs to LDs. For this, hcDIGs derived from [ $^{14}$ C]inositol-labeled control or palmitate-, glimepiride-, and GO-treated adipocytes were incubated with cytosol, FAs, an ATP-regenerating system, and [ $^3$ H]glycerol-3-phosphate and then separated from the putatively formed LDs by sucrose gradient centrifugation. Fractions of different buoyant density were analyzed for the presence of radiolabeled Gce1 and CD73 by affinity purification and subsequent phosphorimaging and of LD marker proteins by immunoblotting and for TAG synthesis (by assaying glycerol-3-phosphate in-

corporation into toluene-extractable lipids) (Fig. 6). A considerable portion of the newly synthesized radiolabeled TAG was recovered with the top fraction ( $d \leq 1.059$  g/ml), which apparently contained LDs according to their content of caveolin-1 and perilipin-A/B. The amount of TAG was significantly higher in palmitate-, glimepiride-, and GO-treated adipocytes than in basal cells and reached the level observed with the bottom fraction ( $d = 1.175$  g/ml), which apparently corresponded to hcDIGs. TAG synthesis by hcDIGs and the distribution of caveolin-1 and perilipin-A/B between the top (LDs) and bottom (hcDIGs) fractions, however, were not significantly affected by suppressed lipolysis (Fig. 6 and data not shown). In contrast, [ $^{14}$ C]inositol-labeled Gce1 and CD73 were predominantly recovered with the LDs or hcDIGs using hcDIGs from palmitate-, glimepiride-, and GO-treated or basal adipocytes, respectively (Fig. 6). Together, the distributions of marker proteins and TAG synthesis capability argue that hcDIGs (bottom fraction) and LDs (top fraction) are efficiently separated from one another by three gradient fractions of intermediate density ( $d = 1.105$ ,  $1.119$ , and  $1.148$ ). Incubation of the cell-free system in the absence of cytosol, glycerol-3-phosphate, or oleoyl-CoA completely abrogated the agent-dependent increases in TAG synthesis and Gce1 amount at LDs (data not shown). These findings suggest that in rat adipocytes LDs equipped with typical LD-associated proteins, such as caveolin and perilipin, the GPI proteins Gce1 and CD73 and TAG-synthesizing enzymes are formed by hcDIGs. This mechanism depends on cytosolic



conditions and then analyzed for the presence of HSL, perilipin-A, caveolin-1 (b), and flotillin-1 (c) by immunoblotting. Chemiluminescent images from a representative experiment repeated once are shown. d, other portions of the hcDIGs, lcDIGs, and LDs were analyzed for cholesterol and TAG synthesis. Quantitative evaluations (means  $\pm$  S.D.,  $n = 3$  independent adipocyte preparations and cholesterol/TAG synthesis measurements) are given. The amounts of cholesterol and TAG synthesis measured with hcDIGs from untreated adipocytes were set at 1. \*, significant difference ( $p < 0.05$ ) compared with the corresponding fraction from untreated adipocytes. ●, significant difference ( $P < 0.05$ ) compared with hcDIGs from the correspondingly treated adipocytes.

factor(s) and ongoing TAG synthesis; is activated by palmitate, glimepiride, and GO action; and can be reconstituted in a cell-free system.

**Role of the GPI Anchor Cleavage in the Translocation of Gce1 and CD73 to LDs.** In basal adipocytes, Gce1 and CD73 are anchored at hcDIGs via covalently linked GPI anchors. These are accessible to cleavage by a plasma membrane GPI-PLC known to be activated by glimepiride (Müller et al., 1993, 1994c; Movahedi and Hooper, 1997). This raised the question of whether the amphiphilic or hydrophilic versions harboring the intact or cleaved GPI anchor (with the phosphoinositol glycan moiety left), respectively, are translocated from hcDIGs to LDs. For this, LD proteins extracted from [ $^{14}$ C]inositol-labeled and palmitate-, GO-, or glimepiride-treated adipocytes were incubated in the absence or presence of bacterial PI-PLC. After their partitioning between aqueous and TX-114 phases, Gce1 was detected by affinity puri-

fication, SDS-PAGE, and phosphorimaging. In palmitate-, GO-, or glimepiride-treated adipocytes, the amounts of amphiphilic Gce1 recovered with the TX-114 phase were 2- to 7-fold higher than in basal cells (Fig. 7). Only low levels of hydrophilic Gce1 were detectable in the aqueous phase in both treated and basal adipocytes. This was confirmed by immunoprecipitation of hydrophilic Gce1 with anti-CRD antibodies, which react with lipolytically cleaved GPI proteins only (Zamze et al., 1988; Müller et al., 1994c). The specificity of the anti-CRD antibodies for the terminal cyclic-1,2-phosphoinositol epitope as generated by bacterial PI-PLC action was demonstrated by inclusion of excess of cyclic-1,2-phosphoinositol, which drastically reduced the amount of immunoprecipitated Gce1 (data not shown). Moreover, amphiphilic rather than hydrophilic CD73 was recovered with LDs from glimepiride-treated adipocytes (data not shown).

LD expression of Gce1 carrying an intact GPI anchor was confirmed by treatment of the LD proteins with bacterial PI-PLC, which led to conversion of the [ $^{14}$ C]inositol-labeled amphiphilic Gce1 into its hydrophilic counterpart, as revealed by TX-114 partitioning and subsequent immunoprecipitation with anti-CRD antibodies (Fig. 7). The generation of hydrophilic Gce1 was abrogated in the presence of the (G)PI-PLC-specific inhibitor GPI2350. Taken together, Gce1 and CD73 harboring the intact GPI anchor rather than their anchorless versions are associated with and translocated to LDs in response to palmitate, glimepiride, and GO action in rat adipocytes. This is in agreement with the requirement of the intact GPI anchor for the successful reconstitution of Gce1 into LDs in vitro (Müller et al., 2008a).

**Role of the Activation of the GPI-PLC for the Translocation of Gce1 and CD73 to LDs.** The GPI anchor of Gce1 and CD73 has recently been demonstrated to be cleaved by the activated GPI-PLC in primary and cultured adipocytes in response to glimepiride (Müller et al., 1993, 1994c). Here, this finding was extended to palmitate and GO action. For this, Gce1 and CD73 were subjected to TX-114 partitioning after their affinity purification from total plasma membranes of [ $^{14}$ C]inositol-labeled and then palmitate-, GO-, or glimepiride-treated adipocytes (Fig. 8). As revealed by the phosphorimages, the levels of [ $^{14}$ C]inositol-labeled hydrophilic Gce1 and CD73 increased significantly with increasing concentrations of palmitate, glimepiride, and GO. The generation of hydrophilic Gce1

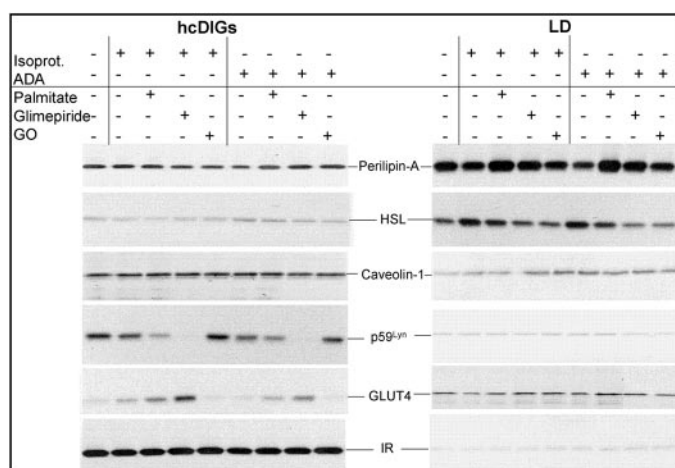


**Fig. 4.** Effect of isoproterenol, ADA, palmitate, glimepiride, and GO on the localization of typical marker proteins for LDs and hcDIGs. Isolated rat adipocytes were incubated (60 min, 37°C) in the absence or presence of palmitate (1 mM), glimepiride (10  $\mu$ M), or GO (100 mU/ml) before the addition of isoproterenol (final concentration, 1  $\mu$ M), ADA (1 U/ml), or buffer alone (basal). After further incubation (20 min), LDs and hcDIGs were prepared from the adipocytes and then used for the extraction and precipitation under denaturing conditions. The solubilized proteins were finally analyzed for the presence of perilipin-A, HSL, caveolin-1, p59<sup>L<sub>yn</sub></sup>, GLUT4, and IR by immunoblotting. Chemiluminescent images from a representative experiment repeated twice are shown.

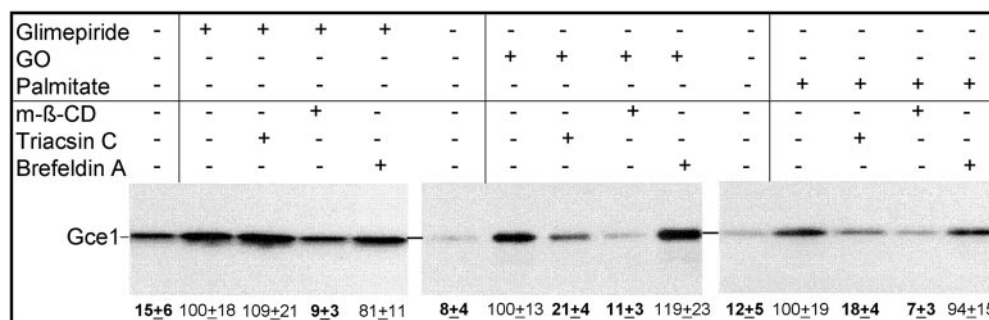


**Fig. 5.** Effect of cholesterol depletion, inhibition of TAG synthesis, and blockade of ER-to-Golgi transport on the steady-state distribution of Gce1. Isolated rat adipocytes were incubated (5 min, 37°C) in the absence or presence of m-β-CD (3.8 mM), Triacsin C (20  $\mu$ M), or brefeldin A (5  $\mu$ g/ml) before treatment with palmitate (final concentration, 1 mM), glimepiride (10  $\mu$ M), or GO (100 mU/ml) as indicated. After further incubation (60 min, 37°C), LDs were prepared from the adipocytes and used for the extraction and precipitation of proteins under native conditions. The solubilized proteins were photoaffinity-labeled with 8-N<sub>3</sub>-[ $^{32}$ P]cAMP for the detection of Gce1, then precipitated under denaturing conditions, and finally separated by SDS-PAGE. Phosphorimages of a typical experiment are shown. Quantitative evaluations (means  $\pm$  S.D.,  $n$  = 3 independent adipocyte preparations and treatments) are given. Boldface numbers indicate significant difference ( $P$  < 0.05) compared with stimulated adipocytes in the absence of m-β-CD, Triacsin C, or brefeldin A set at 100.

and CD73 was completely blocked by the GPI-PLC inhibitor GPI2350. These findings and the apparent retention of the (radiolabeled) inositol residue by hydrophilic Gce1 and CD73 (most likely within the phosphoinositol glycan moiety at the carboxyl terminus of the polypeptide portion) (Fig. 8) strongly argue for lipolytic cleavage of their GPI anchors, most likely by the GPI-PLC. The  $EC_{50}$  values of palmitate, glimepiride, and GO as well as their relative potencies (GO > glimepiride > palmitate) for stimulation of the GPI-PLC (Fig. 8) are well correlated to those for the translocation of Gce1 and CD73 proteins and PDE and 5'-Nuc activities from hcDIGs to LDs (Fig. 1). This raised the question about the putative role of the GPI-PLC in GPI protein translocation.

For study, hcDIGs and LDs were prepared from rat adipocytes that had been treated with palmitate, glimepiride, and GO in the absence or presence of GPI2350 and then analyzed for the presence of amphiphilic or hydrophilic Gce1 by photoaffinity labeling and subsequent TX-114 partitioning. As expected, the phosphorimages demonstrated palmitate-,

glimepiride-, and GO-induced increases and decreases in amphiphilic Gce1 at LDs and hcDIGs, respectively, and significant increases in hydrophilic Gce1 at hcDIGs. The apparent retention of the anchorless version of Gce1 at hcDIGs rather than its translocation to LDs is in agreement with the above findings. It is noteworthy that the addition of GPI2350 abrogated the agent-dependent translocation of amphiphilic Gce1 to LDs and completely eliminated hydrophilic Gce1 from hcDIGs. In contrast, an inactive version of GPI2350, GPI2349 (Müller et al., 2005), was completely ineffective (data not shown), arguing for efficient blockade of the GPI-PLC by GPI2350. This demonstrates the involvement of the GPI-PLC in the palmitate-, glimepiride-, and GO-induced lipolytic cleavage of GPI proteins and the translocation of their anchor-harboring versions from hcDIGs to LDs. The low amount of Gce1 cleaved by the GPI-PLC in untreated adipocytes was apparently not sufficient for triggering detectable translocation of its anchor-containing counterpart (Fig. 9).

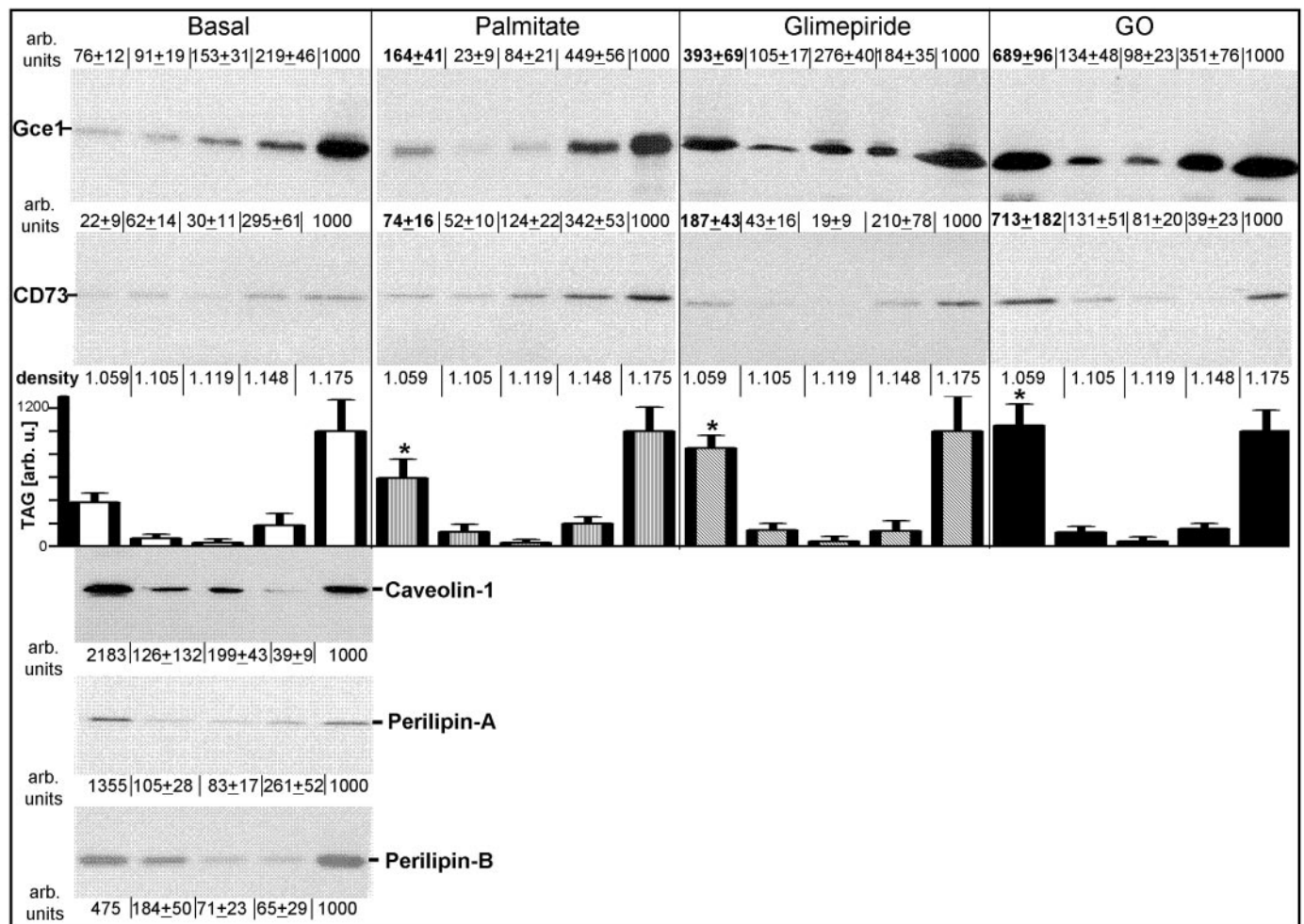


**Fig. 6.** Translocation of Gce1 and CD73 from hcDIGs to LDs in a cell-free system. Isolated rat adipocytes were metabolically labeled (60 min) with [ $m$ yo- $^{14}$ C]inositol and then incubated (4 h, 37°C) in the absence (basal) or presence of palmitate (1 mM), glimepiride (10  $\mu$ M), or GO (100 mU/ml). Thereafter, hcDIGs were prepared from the adipocytes. Portions were incubated (60 min, 37°C) with cytosol, oleoyl-CoA, oleate, CoA, an ATP-regenerating system, and [ $^3$ H]glycerol-3-phosphate as described under *Materials and Methods* and then subjected to sucrose gradient centrifugation. Portions (0.2 ml) of the five fractions obtained were analyzed for TAG synthesis. Other portions were precipitated under denaturing (0.1 ml) or native (0.5 ml) conditions and then analyzed for the presence of caveolin-1 and perilipin-A/B by immunoblotting or of Gce1 and CD73 by affinity purification and subsequent SDS-PAGE. Chemiluminescent and phosphorimages of a representative experiment are shown. Quantitative evaluations (mean  $\pm$  S.D.,  $n = 4$  independent adipocyte preparations/incubations) of the amounts of Gce1, CD73, caveolin-1, perilipin-A/B, and TAG-synthesizing enzymes are given and set at 1000 for the bottom fraction ( $d = 1.175$ ) for each incubation condition. Boldface numbers/\* indicate significant difference ( $P < 0.05$ ) compared with the top fraction ( $d = 1.059$ ) from control adipocytes.

Because Gce1 and CD73 bind and degrade cAMP and AMP, respectively, occupancy of their substrate binding sites could modulate their translocation from hcDIGs to LDs. This was tested by incubation of isolated rat adipocytes with excess of cAMP or AMP or their nonhydrolyzable analogs, Br-cAMPS or AMPCP, before challenge with palmitate, glimepiride, or GO. LDs and hcDIGs were prepared and then assayed for the presence of Gce1 and CD73 by photoaffinity labeling and TX-114 partitioning of the extracted proteins. The phosphorimages (Fig. 10A) demonstrated that excess of Br-cAMPS or AMPCP or, most effectively, a combination thereof significantly reduced, whereas excess of cAMP or AMP increased the amounts of

amphiphilic and hydrophilic Gce1 and CD73 at LDs and hcDIGs, respectively, in palmitate-, glimepiride-, and GO-treated adipocytes. ATP or adenosine did not affect the agent-dependent lipolytic cleavage and translocation of Gce1 and CD73 (data not shown). High concentrations of Br-cAMPS, AMPCP, cAMP, and AMP did not affect the GPI-PLC activity of isolated rat adipocyte hcDIGs when measured in vitro with bovine brain acetylcholinesterase as the GPI protein substrate arguing against direct inhibition of the GPI-PLC by (c)AMP analogs (data not shown). Measurement of the cAMP-to-adenosine conversion by isolated LDs (Fig. 10B) revealed that exogenously added cAMP and AMP significantly

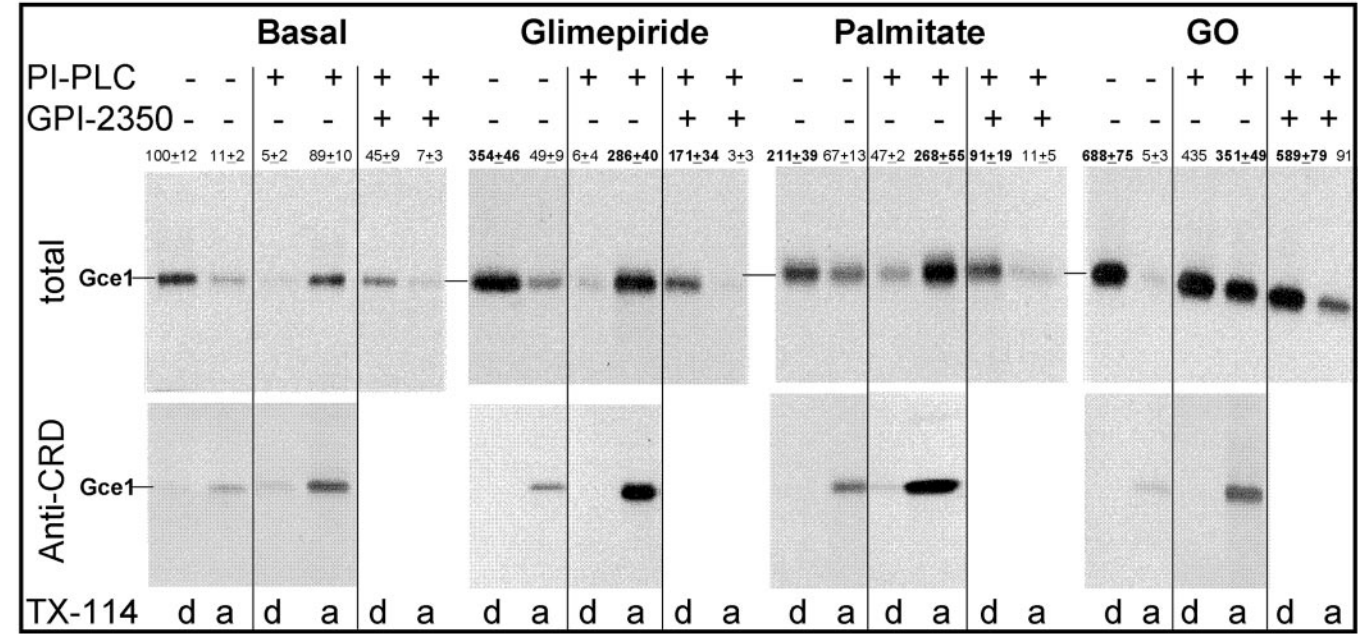


**Fig. 7.** Effect of palmitate, glimepiride, and GO action on the steady-state distribution of anchor-containing and anchor-less Gce1 at LDs. Isolated rat adipocytes were metabolically labeled (60 min) with [*m*yo-<sup>14</sup>C]inositol and then incubated (60 min, 37°C) in the absence (basal) or presence of palmitate (1 mM), glimepiride (10 μM), or GO (100 mU/ml). Thereafter, LDs were prepared from the adipocytes for the extraction and precipitation of proteins under native conditions. The solubilized proteins were treated without or with PI-PLC (*Bacillus cereus*) in the absence or presence of GPI2350 (100 μM). After TX-114 partitioning, the proteins recovered from the aqueous (a) and TX-114 (d) phases were precipitated under native conditions. After solubilization of the proteins, Gce1 was affinity-purified. Portions of the eluted Gce1 were analyzed by SDS-PAGE (total). Other portions were immunoprecipitated with anti-CRD antibodies before SDS-PAGE (anti-CRD). The phosphorimages of a representative experiment are shown. Quantitative evaluations (mean ± S.D., *n* = 4 independent adipocyte preparations/incubations) are given. The amounts of Gce1 not treated with PI-PLC and recovered with the TX-114 phase from LDs of basal adipocytes were set at 100. Boldface numbers indicate significant difference (*P* < 0.05) compared with the correspondingly treated Gce1 recovered from the corresponding phase of basal adipocytes.

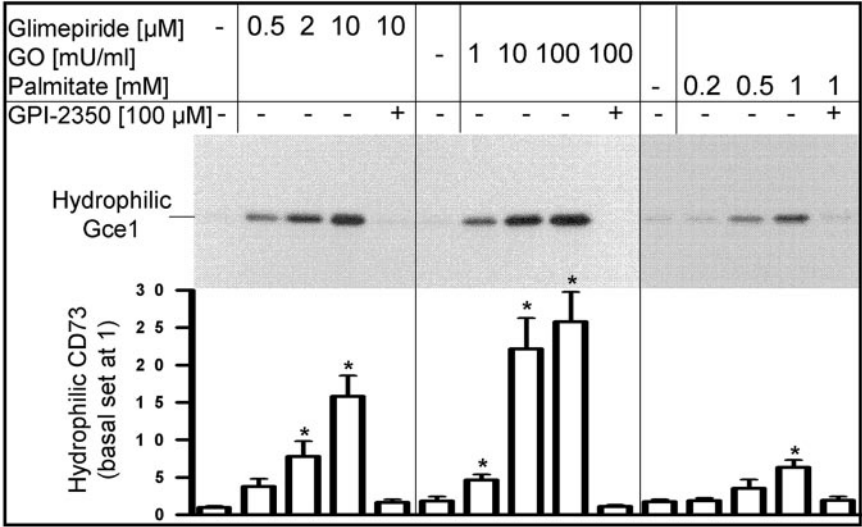


**Fig. 8.** Effect of palmitate, glimepiride, and GO action on the lipolytic cleavage Gce1 and CD73. Isolated rat adipocytes were metabolically labeled (60 min) with [*m*yo-<sup>14</sup>C]inositol and then incubated (5 min, 37°C) in the absence or presence of GPI2350 (100 μM) before the addition of increasing concentrations of palmitate, glimepiride, or GO. After further incubation (60 min, 37°C), plasma membranes were prepared from the adipocytes and subjected to TX-114 partitioning. Proteins recovered with the aqueous phase were precipitated under native conditions. Gce1 and CD73 were affinity-purified from the solubilized proteins and after elution were analyzed by SDS-PAGE. Phosphorimages of a representative experiment are shown (for Gce1 only). Quantitative evaluations (means ± S.D., *n* = 4 independent adipocyte preparations and metabolic labelings) are given (for CD73 only) with the amount of hydrophilic CD73 recovered with plasma membranes of untreated adipocytes set at 1. \*, significant difference (*P* < 0.05) compared with the corresponding untreated adipocytes.

enhanced and SP-8-Br-cAMPs and AMPCP diminished the palmitate-, glimepiride-, and GO-induced up-regulation of the cAMP-degrading activity at LDs. Again, ATP and adenosine were ineffective (data not shown). These findings demonstrate that occupancy of the GPI proteins Gce1 and CD73 with non-hydrolyzable substrate analogs and the authentic substrates impairs and favors, respectively, their agent-induced translocation from hcDIGs to LDs in rat adipocytes.

It is remarkable that Br-cAMPS alone impaired the redistribution of CD73, and vice versa, AMPCP alone impaired the redistribution of Gce1 (Fig. 10A). These findings argue for interference of nucleotide binding to and/or inhibition of Gce1 or CD73 with a common translocation apparatus that may be shared by other GPI proteins too and rely on their aggregation/complex formation. On the other hand, on the basis of the limited membrane permeability of the (c)AMP analogs used, control of the translocation by the (c)AMP-dependent protein kinases cannot be completely dismissed.

**Role of the GPI-PLC and Translocation of Gce1 and CD73 to LDs for Inhibition of Lipolysis by Palmitate, Glimepiride, and  $H_2O_2$ .** The role of the stimulation of the GPI-PLC and GPI protein translocation by palmitate, glimepiride, and GO action for their antilipolytic activity in rat adipocytes was studied by inhibition of the GPI-PLC with GPI2350 and activation or inhibition of the Gce1/CD73 translocation with excess of cAMP/AMP or Br-cAMPS/AMPCP, respectively. Analysis of the glycerol and FA release (Fig. 11) and the amount of LD-associated HSL (Fig. 12) revealed that inhibition of the GPI-PLC and GPI protein translocation does not affect basal and isoproterenol-induced lipolysis per se (data not shown). However, GPI2350 (but not GPI2349), Br-cAMPS, and AMPCP completely abrogated the inhibition of the isoproterenol-stimulated lipolysis (Fig. 11) and translocation of HSL to LDs (Fig. 12) in response to palmitate, glimepiride, and GO action but not to insulin. In contrast, exogenous cAMP and AMP alone or in combination with identical concentrations of Br-cAMPS and AMPCP did not

compromise lipolysis inhibition by either agent. Thus, the molecular mechanism for the antilipolytic activity of palmitate, glimepiride, and GO action in rat adipocytes apparently relies on activation of the GPI-PLC and the translocation of Gce1 and CD73 and thereby differs from that engaged by insulin.

## Discussion

The following experimental evidence reported in this study strongly argues for the regulated translocation of the GPI proteins Gce1 and CD73, which in a concerted action convert cAMP into adenosine (Müller et al., 2008a) from DIGs to LDs in primary rat adipocytes: 1) disruption of plasma membrane DIGs upon cholesterol depletion from intact adipocytes abrogates palmitate-, glimepiride-, and  $H_2O_2$ -triggered conversion of cAMP to adenosine by isolated LDs (Table 1) and the up-regulation of Gce1 protein expression at LDs (Fig. 5); 2) the steady-state distributions of the Gce1 and CD73 proteins and of their intrinsic PDE and 5'-Nuc activities are shifted from hcDIGs, their predominant localization in the basal state, to LD upon challenge of the adipocytes with palmitate, glimepiride, and  $H_2O_2$  (Figs. 1 and 3); 3) pulse and equilibrium labeling of the GPI anchors of Gce1 and CD73 with the anchor constituent inositol is compatible with a precursor-product relationship between the GPI proteins recovered with hcDIGs and LDs in both basal and palmitate-, glimepiride-, and  $H_2O_2$ -treated adipocytes. However, in the treated adipocytes, less pronounced increases and shorter chase times for Gce1 and CD73 at hcDIGs during pulse and equilibrium labeling, respectively, and more pronounced increases at LDs during both pulse and equilibrium labeling were observed (Fig. 2); 4) the translocation from hcDIGs to LDs is specific for Gce1 and CD73 because the distribution of typical marker proteins for DIGs, caveolae, and LDs, such as caveolin, perilipin, HSL, and TAG-synthesizing enzymes, is not affected by palmitate, glimepiride, and  $H_2O_2$  (Figs. 3, B

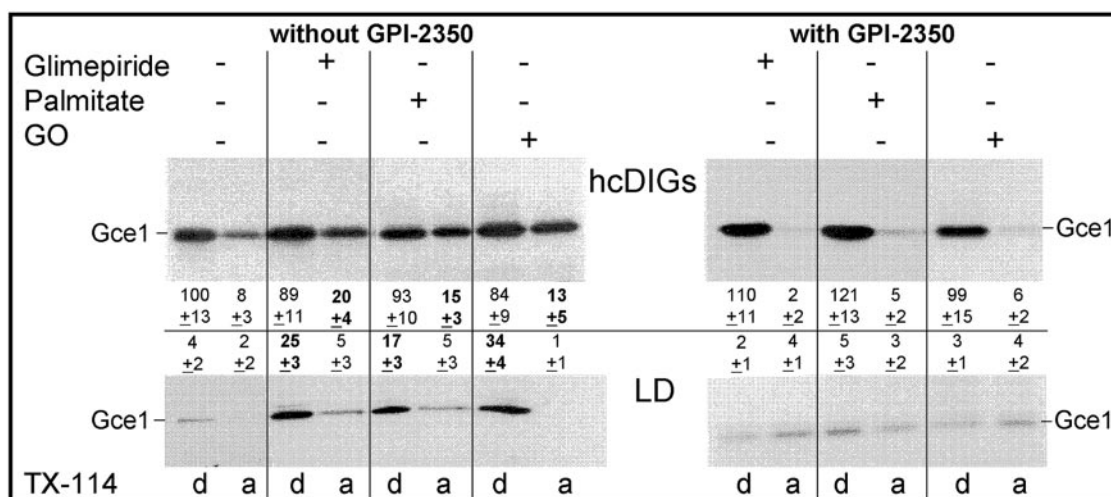


**Fig. 9.** Effect of inhibition of the GPI-PLC on the palmitate-, glimepiride-, and GO-induced translocation of Gce1. Isolated rat adipocytes were incubated (5 min, 37°C) in the absence or presence of GPI2350 (100  $\mu$ M) before the addition of palmitate (final concentration, 1 mM), glimepiride (10  $\mu$ M), GO (100 mU/ml), or buffer. After further incubation (20 min, 37°C), hcDIGs and LDs were prepared from the adipocytes for the extraction and precipitation of proteins under native conditions. Solubilized proteins were photoaffinity-labeled with 8- $N_3$ -[ $^{32}$ P]cAMP, partitioned between aqueous (a) and TX-114 (d) phases, then precipitated under denaturing conditions, and finally analyzed by SDS-PAGE. The phosphorimages of a representative experiment are shown. Quantitative evaluations (means  $\pm$  S.D.,  $n = 3$  independent adipocyte preparations/incubations) are given with the amount of amphiphilic Gce1 recovered with the hcDIGs from untreated adipocytes in the absence of GPI2350 set at 100. Boldface numbers indicate significant difference ( $P < 0.05$ ) compared with the aqueous phase of hcDIGs or detergent phase of LDs, respectively, from untreated adipocytes.

and C, and 4); and 5) the translocation reaction can be reconstituted in a cell-free system consisting of hcDIGs, cytosolic factors, ATP, and precursors of TAG synthesis (Fig. 6).

**Role of the GPI Anchor (Cleavage) for the Translocation of Gce1 and CD73.** The following findings suggest that GPI-anchored rather than lipolytically cleaved Gce1 and CD73 are translocated from hcDIGs to LDs: 1) Gce1 does not get rid of its GPI anchor during translocation to LDs because it retains its amphiphilic nature and displays the anti-CRD epitope upon cleavage by the PI-PLC, which are both char-

acteristic for modification by the intact GPI structure (Fig. 7); and 2) Gce1p from yeast harboring the intact rather than the lipolytically cleaved GPI anchor associates with LDs in vitro and confers PDE activity onto LDs (Müller et al., 2008a). Thus, GPI anchorage seems to ensure stable association of Gce1 and CD73 with LDs.

We were surprised to find that although Gce1 and CD73 with intact GPI anchor are translocated to LDs, GPI-PLC action seems to be required for their palmitate-, glimepiride-, and  $H_2O_2$ -induced translocation based on the following findings: 1) palmitate, glimepiride, and  $H_2O_2$  induce GPI anchor cleavage of Gce1 and CD73 by the GPI-PLC located at the plasma membrane of rat adipocytes (Fig. 8); 2) Gce1 with cleaved GPI anchor generated in response to these agents accumulates at the hcDIGs rather than at the LDs (Fig. 9); 3) inhibition of the GPI-PLC leads to accumulation of Gce1 harboring the intact GPI anchor at hcDIGs (Fig. 9); and 4) impairment of the palmitate-, glimepiride-, or  $H_2O_2$ -induced generation of Gce1 and CD73 with cleaved GPI anchor at hcDIGs by nonhydrolyzable (c)AMP analogs is correlated well to the reduced appearance of their anchor-containing versions (Fig. 10A) and their intrinsic cAMP-to-adenosine conversion activity (Fig. 10B) at LDs. Taken together, we concluded that challenge of rat adipocytes with palmitate, glimepiride, and  $H_2O_2$  causes 1) cleavage of the GPI anchors

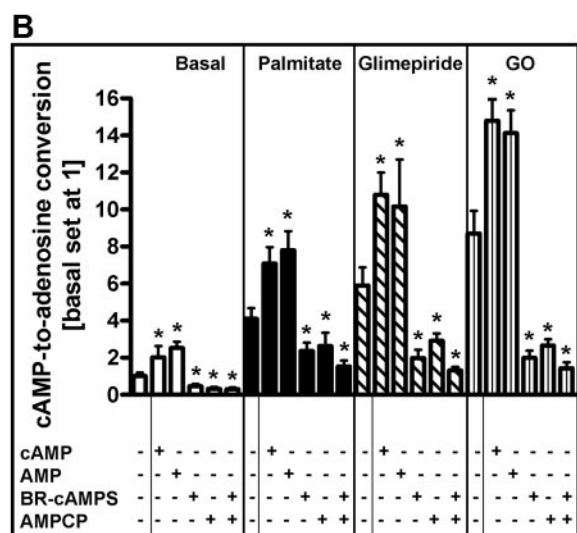
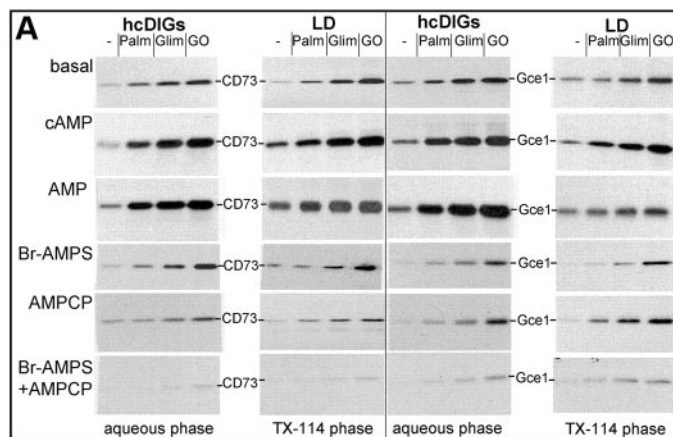


**Fig. 10.** Effect of (c)AMP and analogs on the palmitate-, glimepiride-, and GO-induced lipolytic cleavage and translocation of Gce1 and CD73. Isolated rat adipocytes were incubated (5 min, 37°C) with cAMP, AMP, Br-cAMPS, and AMPCP or combinations thereof (100  $\mu$ M each) before the addition of palmitate (final concentration, 1 mM), glimepiride (10  $\mu$ M), GO (100 mU/ml), or buffer (basal) as indicated. After further incubation (60 min, 37°C), hcDIGs and LDs were prepared from the adipocytes for the extraction and precipitation of proteins under native conditions. Portions of the solubilized proteins were photoaffinity-labeled with 8-N<sub>3</sub>-[<sup>32</sup>P]cAMP or [<sup>14</sup>C]5'-FSBA. After TX-114 partitioning, proteins recovered from the aqueous phases (hcDIGs only) and TX-114 phases (LDs only) were precipitated under denaturing conditions and then analyzed by SDS-PAGE. Phosphorimages of a representative experiment are shown repeated once with similar results (A). Other portions of the solubilized proteins prepared from the LDs were assayed for cAMP-to-adenosine conversion (B). Quantitative evaluations (means  $\pm$  S.D.,  $n = 4$  independent adipocyte preparations/incubations) are given with the cAMP-to-adenosine conversion by LDs from basal adipocytes incubated in the absence of (c)AMP analogs was set at 1. \*, significant difference ( $P < 0.05$ ) compared with the correspondingly treated or basal adipocytes in the absence of the (c)AMP analogs.

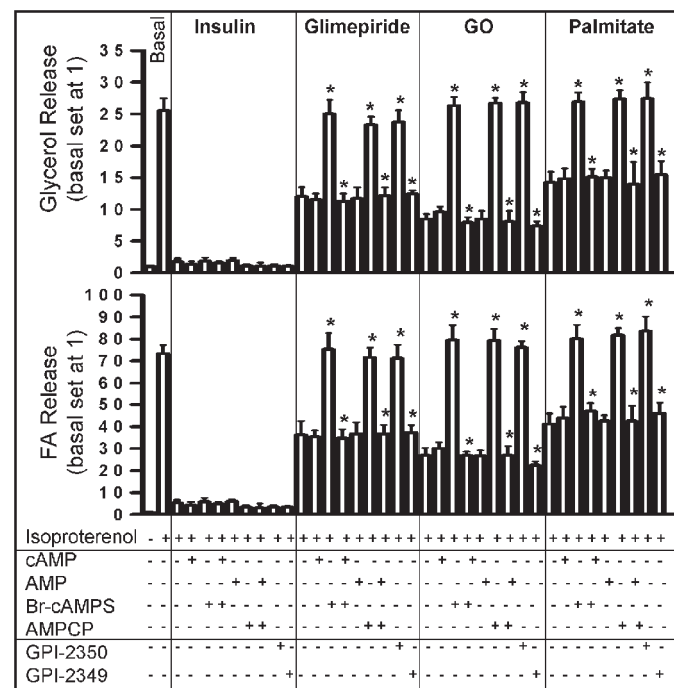


**Fig. 11.** Effect of inhibition of the GPI-PLC and GPI protein translocation on lipolysis inhibition by insulin, palmitate, glimepiride, and GO. Isolated rat adipocytes were incubated (5 min, 37°C) in the absence or presence of GPI2350 (100  $\mu$ M), GPI2349 (100  $\mu$ M), Br-cAMPS, AMPCP, cAMP, or AMP (100  $\mu$ M each) before the addition of insulin (final concentration, 5 nM), palmitate (1 mM), glimepiride (10  $\mu$ M), GO (100 mU/ml), or buffer (basal). After further incubation (30 min), isoproterenol (final concentration, 1  $\mu$ M) or buffer was added. After incubation (90 min), the medium was separated from the adipocytes and analyzed for glycerol and FA release (means  $\pm$  S.D.,  $n = 5$  independent adipocyte preparations/incubations) with the values obtained with basal adipocytes in the absence of isoproterenol/(c)AMP analog/inhibitor set at 1. \*, significant difference ( $P < 0.05$ ) compared with the correspondingly treated isoproterenol-stimulated adipocytes in the absence of (c)AMP analog or inhibitor.

of Gce1 and CD73 by the activated GPI-PLC; 2) retention at hcDIGs of Gce1 and CD73 with cleaved GPI anchor, presumably upon interaction of the generated phosphoinositol glycan moiety with a recently discovered receptor at hcDIGs (Müller et al., 2002a); and 3) translocation of Gce1 and CD73 with intact GPI anchor from hcDIGs to LDs.

**Mechanism of GPI Protein Translocation to LDs.** The findings of the regulated translocation of the GPI proteins Gce1 and CD73 from plasma membrane hcDIGs to cytosolic LDs raises the intriguing question about the molecular mechanism involved. Three models can be envisaged that differ predominantly in the sites of TAG synthesis and LD formation: 1) translocation of Gce1 and CD73 to the ER by vesicular trafficking and subsequently to LDs as they are formed at and released from the ER; 2) translocation alone or accompanied by FA molecules, which have been taken up at DIGs, to pre-existing cytosolic LDs; and 3) incorporation into peripheral LDs as these are formed at and released from plasma membrane DIGs followed by fusion with central LDs.

Compatible with the currently widely accepted model for LD biogenesis involving vesicular budding of LDs from TAG-surrounding ER membrane leaflets (Wolins et al., 2006) and the appearance at LDs of transient ER proteins, such as the caveolins (Robenek et al., 2005a,b) and the GPI proteins Gce1 and CD73, as reported here, are the recent findings of the presence of ribosomes, ER-like membranes, and many ER-specific membrane and luminal proteins at the LDs of U937 human monocytes (Wan et al., 2007). However, brefeldin A, which blocks vesicular trafficking of proteins from the ER to the Golgi apparatus, also in adipocytes, does not impair the palmitate-, glimepiride-, and H<sub>2</sub>O<sub>2</sub>-triggered translocation of Gce1 and CD73 from hcDIGs to LDs (Fig. 5). Moreover, endocytic movement of Gce1 and CD73 to the ER would result in luminal orientation of their protein moieties and insertion of their GPI anchors into the luminal ER membrane leaflet. This topology is incompatible with budding of the LDs together with the GPI proteins incorporated into their phospholipid monolayer shell from the cytoplasmic ER membrane leaflet. Taken together, vesicular trafficking between the plasma membrane and the ER, and subsequent

budding of LDs from the ER does not seem to be involved in the translocation of Gce1 and CD73 to LDs in response to palmitate, glimepiride, or H<sub>2</sub>O<sub>2</sub>.

Regarding nonvesicular mechanisms for the direct translocation of GPI proteins from hcDIGs to pre-existing cytosolic LDs, it may be of relevance that PAT family protein members, such as perilipin, which are typical LD-associated proteins, have been identified recently as integral components of the plasma membrane (Robenek et al., 2005a; Aboulaich et al., 2006). Moreover, typical DIG-associated proteins such as caveolin and stomatin have been recovered previously with LDs (Umlauf et al., 2004; Robenek et al., 2005b), hinting to the existence of (transient) contacts or interactions between plasma membrane DIGs and LDs. Thus, adipocyte LDs may recruit their PAT proteins and caveolin-1 by direct interaction with specialized DIGs of the plasma membrane. This "imprinting" mechanism may be facilitated by the short distance (~0.5  $\mu$ m) between the adipocyte plasma membrane and the cytosolic LDs separated by a thin film of cytoplasm only. On the other hand, the existence of a translocation channel between caveolae/DIGs and LDs may be envisaged. In insulin-stimulated adipocytes, fluorescent FAs have been demonstrated to accumulate in caveolin-containing large (>1  $\mu$ m) fluorescent bulbs at the plasma membrane and subsequently to penetrate and dissolve into the large cytosolic LDs of the cell (Ost et al., 2005; Ortegren et al., 2006). It is therefore conceivable that FA molecules are transferred from their site of uptake at plasma membrane caveolae/DIGs in concert with a subset of GPI proteins in micellar structures via the translocation channel to the sites of their incorporation into and storage as TAG, the cytosolic LDs. This mechanism would lead to a direct flow of FAs from the caveolae/DIGs to the LDs, as was indeed inferred from fluorescence microscopy data (Ortegren et al., 2006), which may be accompanied by the brefeldin A-insensitive cotranslocation of Gce1 and CD73 from DIGs to LDs.

An alternative vesicular trafficking-independent mechanism of GPI protein translocation from DIGs to specialized peripheral LDs on the basis of their direct formation at and release from DIGs has been supported recently by the iden-

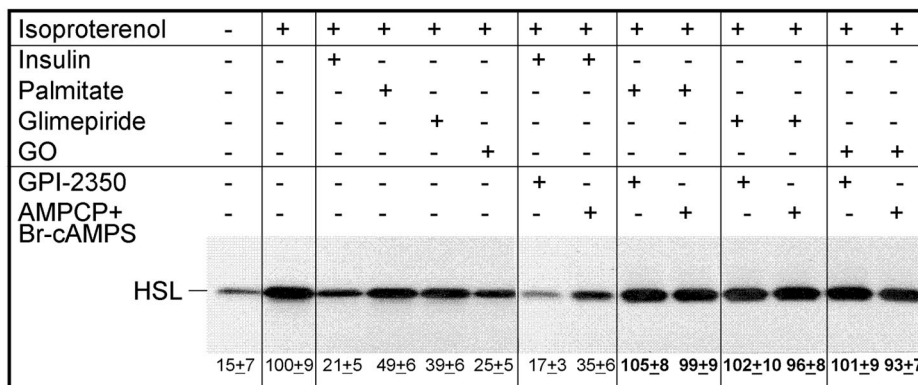


**Fig. 12.** Effect of inhibition of the GPI-PLC and GPI protein translocation on the inhibition of HSL translocation by insulin, palmitate, glimepiride, and GO. Isolated rat adipocytes were incubated (5 min, 37°C) in the absence or presence of GPI2350 (100  $\mu$ M) or AMPCP plus Br-cAMPS (100  $\mu$ M each) before the addition of insulin (final concentration, 5 nM), palmitate (1 mM), glimepiride (10  $\mu$ M), GO (100 mU/ml), or buffer. After further incubation (30 min), isoproterenol (final concentration, 1  $\mu$ M) or buffer was added and the incubation continued (20 min). LDs were prepared from the adipocytes and used for the extraction and precipitation of proteins under denaturing conditions. Thereafter, the solubilized proteins were immunoblotted for HSL. Chemiluminescent images of a representative experiment are shown. Quantitative evaluations (means  $\pm$  S.D.,  $n = 3$  independent adipocyte preparations/incubations) are given with the amount of HSL recovered with LDs from isoproterenol-treated adipocytes in the absence of antilipolytic challenge/(c)AMP analog/GPI2350 set at 100. Boldface numbers indicate significant difference ( $P < 0.05$ ) compared with the correspondingly treated adipocytes in the absence of (c)AMP analog/GPI2350.

tification of a subclass of high-buoyant density and apparently closed plasma membrane-associated caveolae in primary rat adipocytes (Ost et al., 2005). These are capable of synthesizing TAG and assembling (a subclass of) LDs as tiny dispersed structures near the cell periphery (Ortegren et al., 2006). The relationship of these high-buoyant density caveolae to the lcDIGs prepared in this study on basis of detergent insolubility, low cholesterol content, and high-buoyant density and identified as the site for the accumulation of Gce1 and CD73 similar to, albeit with lower efficacy than, LD (Fig. 3, A and B) remains to be clarified. lcDIGs operating as the site for the formation of GPI protein-harboring LDs are compatible with the findings described here using a cell-free system: 1) incubation of isolated caveolin-containing hcDIGs with cytosol, ATP, and components required for TAG synthesis leads to the formation of typical LDs (as judged from buoyant density, accumulation of TAG, presence of caveolin-1, and perilipin-A/B), which harbor Gce1 (Fig. 6); and 2) in vitro GPI proteins undergo an exchange between distinct LDs or GPI protein-harboring LDs and manage to fuse with each other in a cytosol- and ATP-dependent process (Müller et al., 2008a). It is tempting to speculate that peripheral LDs formed at DIGs undergoes fusion with the ER-derived central LDs during LD maturation accompanied by sequential translocation of a subset of GPI proteins from hcDIGs to lcDIG-derived LDs to ER-derived LDs. In conclusion, evidence available so far favors the translocation of GPI proteins from hcDIGs to LDs involving the formation of peripheral LDs at DIGs of the adipocyte plasma membrane.

TAG synthesis and LD formation by specialized plasma membrane DIGs may be of advantage for adipocytes because they are faced with a massive influx of potentially lethal FAs. Because of their pronounced detergent resistance, the caveolin-containing DIGs/caveolae are adapted to cope with the detergent properties of FAs by promoting the de novo synthesis of TAG from FAs and glycerol-3-phosphate in the plasma membrane of primary adipocytes. Compatible with this physiological role of adipocyte DIGs are the findings that 1) caveolin-1, a major component of hcDIGs, has been shown to bind FAs (Trigatti et al., 1999); 2) overexpression of caveolin-1 in human embryonic kidney 293 cells enhances the transmembrane flux of FAs (Meshulam et al., 2006); and 3) uptake of FAs by the adipocytes seems to be regulated at the level of its conversion into TAG, at least at high concentrations (Mashek and Coleman, 2006). Thus, TAG synthesis and LD formation at hcDIGs/caveolae of the adipocyte plasma membrane could ensure rapid and efficient sequestration of FAs, at least under certain physiological (excess of FAs or reactive oxygen species) or pharmacological conditions (administration of glimepiride). Up-regulation of the translocation of the cAMP-to-adenosine conversion machinery consisting of the PDE, Gce1, and the 5'-Nuc, CD73, from hcDIGs to the LDs under these conditions may facilitate the formation of LDs and improve their resistance against cAMP-dependent lipolytic attack involving protein kinase A-activated lipases, such as HSL (Müller et al., 2008b). It is tempting to speculate that the transfer of Gce1 and CD73 from hcDIG-derived peripheral LDs to ER-derived central LDs in the course of their subsequent fusion may guarantee the coordination of LD biogenesis between both sites in the case of excessive burden of the adipocytes with FAs or reactive oxygen species. Studies are in progress to elucidate the primary

molecular mechanism(s) of GPI-PLC activation and GPI protein translocation putatively shared by  $H_2O_2$ , palmitate, and glimepiride. They may provide novel target(s) for the treatment of metabolic diseases, such as type II diabetes and hyperlipidemia, which are believed to rely on unrestrained lipolysis and impaired LD formation in adipocytes (Unger, 2002).

## References

- Aboulaich N, Vener AV, and Stralfors P (2006) Hormonal control of reversible translocation of perilipin B to the plasma membrane in primary human adipocytes. *J Biol Chem* **281**:11446–11449.
- Anderson RGW (1998) The caveolae membrane system. *Annu Rev Biochem* **67**:199–225.
- Avruch J and Wallach DFH (1971) Preparation and properties of plasma membrane and endoplasmic reticulum fragments from isolated rat fat cells. *Biochim Biophys Acta* **233**:334–347.
- Bordier C (1981) Phase separation of integral membrane proteins in Triton X-114 solution. *J Biol Chem* **256**:1604–1607.
- Brown DA and Rose JK (1992) Sorting of GPI-anchored proteins to glycolipid-enriched membrane subdomains during transport to the apical cell surface. *Cell* **68**:533–544.
- Fujimoto T, Kogo H, Ishiguro K, Tauchi K, and Nomura R (2001) Caveolin-2 is targeted to lipid droplets, a new 'membrane domain' in the cell. *J Cell Biol* **152**:1079–1085.
- Hansen RS, Charbonneau H, and Beavo JA (1982) Purification of two calcium/calmodulin-dependent forms of cyclic nucleotide phosphodiesterase by using conformation-specific monoclonal antibody chromatography. *Proc Natl Acad Sci U S A* **79**:2788–2792.
- Hanzal-Bayer MF and Hancock JF (2007) Lipid rafts and membrane traffic. *FEBS Lett* **581**:2098–2104.
- Klip A, Ramlal T, Douen AG, Burdett E, Young D, and Cartree GD (1988) Insulin-induced decrease in 5-nucleotidase activity in skeletal muscle membranes. *FEBS Lett* **238**:419–423.
- Langhorst F, Reuter A, and Stuermer CA (2005) Scaffolding microdomains and beyond the function of reggie/flotillin proteins. *Cell Mol Life Sci* **62**:2228–2240.
- Londos C, Sztalryd C, Tansey JT, and Kimmel AR (2005) Role of PAT proteins in lipid metabolism. *Biochimie* **87**:45–49.
- Martin S and Parton G (2005) Caveolin, cholesterol, and lipid bodies. *Semin Cell Dev Biol* **16**:163–174.
- Mashek DG and Coleman RA (2006) Cellular fatty acid uptake: the contribution of metabolism. *Curr Opin Lipidol* **17**:274–278.
- Meshulam T, Simard JR, Wharton J, Hamilton JA, and Pilch PF (2006) Role of caveolin-1 and cholesterol in transmembrane fatty acid movement. *Biochemistry* **45**:2882–2893.
- Movahedi S and Hooper N (1997) Insulin stimulates the release of the glycosyl phosphatidylinositol-anchored membrane dipeptidase from 3T3-L1 adipocytes through the action of a phospholipase C. *Biochem J* **326**:531–537.
- Müller G (2002) Dynamics of plasma membrane microdomains and cross-talk to the insulin signalling cascade. *FEBS Lett* **531**:81–87.
- Müller G, Dearey EA, Korndörfer A, and Bandlow W (1994a) Stimulation of a glycosyl phosphatidylinositol-specific phospholipase by insulin and the sulfonylurea, glimepiride, in rat adipocytes depends on increased glucose transport. *J Cell Biol* **126**:1267–1276.
- Müller G, Dearey EA, and Pünter J (1993) The sulphonylurea drug, glimepiride, stimulates release of glycosylphosphatidylinositol-anchored plasma-membrane proteins from 3T3 adipocytes. *Biochem J* **289**:509–521.
- Müller G, Hanekop N, Kramer W, Bandlow W, and Frick W (2002a) Interaction of phosphoinositidylglycan(-peptides) with plasma membrane lipid rafts of rat adipocytes. *Arch Biochem Biophys* **408**:17–32.
- Müller G, Hanekop N, Wied S, and Frick W (2002b) Cholesterol depletion blocks redistribution of lipid raft components and insulin-mimetic signaling by glimepiride and phosphoinositidylglycans in rat adipocytes. *Mol Med* **8**:120–136.
- Müller G, Jordan H, Jung C, Kleine H, and Petry S (2003) Analysis of lipolysis in adipocytes using a fluorescent fatty acid derivative. *Biochimie* **85**:1245–1256.
- Müller G, Jung C, Wied S, Welte S, Jordan H, and Frick W (2001) Redistribution of glycolipid raft domain components induces insulin-mimetic signaling in rat adipocytes. *Mol Cell Biol* **21**:4553–4567.
- Müller G, Korndörfer K, Saar K, Karbe-Thönges B, Fasold H, and Müllner S (1994b) 4'-Amino-benzamido-taurolcholic acid selectively solubilizes glycosyl-phosphatidylinositol-anchored membrane proteins and improves lipolytic cleavage of their membrane anchors by specific phospholipases. *Arch Biochem Biophys* **309**:329–340.
- Müller G, Over S, Wied S, and Frick W (2008a) Association of (c) AMP-degrading glycosylphosphatidylinositol-anchored proteins with lipid droplets is induced by palmitate,  $H_2O_2$  and the sulfonylurea drug, glimepiride, in rat adipocytes. *Biochemistry* **47**:1274–1287.
- Müller G, Schulz A, Wied S, and Frick W (2005) Regulation of lipid raft proteins by glimepiride- and insulin-induced glycosylphosphatidylinositol-specific phospholipase C in rat adipocytes. *Biochem Pharmacol* **69**:761–780.
- Müller G, Wetekam EA, Jung C, and Bandlow W (1994c) Membrane association of lipoprotein lipase and a cAMP-binding ectoprotein in rat adipocytes. *Biochemistry* **33**:12149–12159.
- Müller G, Wied S, Over S, and Frick W (2008b) Inhibition of lipolysis by palmitate,  $H_2O_2$  and the sulfonylurea drug, glimepiride, in rat adipocytes depends on cAMP degradation by lipid droplets. *Biochemistry* **47**:1259–1273.
- Ortegren U, Yin L, Ost A, Karlsson M, Nystrom FH, Gustavsson J, and Stralfors P

- (2006) Separation and characterization of caveolae subclasses in the plasma membrane of primary adipocytes; segregation of specific proteins and functions. *FEBS J* **273**:3381–3392.
- Ost A, Ortegren U, Gustavsson J, Nystrom FH, and Stralfors P (2005) Triacylglycerol is synthesized in a specific subclass of caveolae in primary adipocytes. *J Biol Chem* **280**:5–8.
- Parton RG, Hanzal-Bayer M, and Hancock JF (2006) Biogenesis of caveolae: a structural model for caveolin-induced domain formation. *J Cell Sci* **119**:787–796.
- Parton RG and Richards AA (2003) Lipid rafts and caveolae as portals for endocytosis: new insights and common mechanisms. *Traffic* **4**:724–738.
- Rajendran L and Simons K (2005) Lipid raft and membrane dynamics. *J Cell Sci* **118**:1099–1102.
- Rietveld A and Simons K (1998) The differential miscibility of lipids as the basis for the formation of functional membrane rafts. *Biochim Biophys Acta* **1376**:467–479.
- Robenek H, Robenek MJ, Buers I, Lorkowski S, Hofnagel O, Troyer D, and Severs NJ (2005a) Lipid droplets gain PAT family proteins by interaction with specialized plasma membrane domains. *J Biol Chem* **280**:26330–26338.
- Robenek H, Robenek MJ, and Troyer D (2005b) PAT family proteins pervade lipid droplet cores. *J Lipid Res* **46**:1331–1338.
- Stochaj U and Mannherz HG (1990) Affinity labelling of 5'-nucleotidases with 5'-*p*-fluorosulphonylbenzoyladenine. *Biochem J* **266**:447–451.
- Trigatti BL, Anderson RG, and Gerber GE (1999) Identification of caveolin-1 as a fatty acid binding protein. *Biochem Biophys Res Commun* **255**:34–39.
- Umlauf E, Csaszar E, Moertelmaier M, Schuetz GJ, Parton RG, and Prohaska R (2004) Association of stomatin with lipid bodies. *J Biol Chem* **279**:23699–23709.
- Unger RH (2002) Lipotoxic diseases. *Annu Rev Med* **53**:319–336.
- Wan HC, Melo RCN, Jin Z, Dvorak AM, and Weller PF (2007) Roles and origins of leukocyte lipid bodies: proteomic and ultrastructural studies. *FASEB J* **21**:167–178.
- Wolins NE, Quaynor BK, Skinner JR, Schoenfish MJ, Tzekov A, and Bickel PE (2005) S3–12, adipophilin, and TIP47 package lipid in adipocytes. *J Biol Chem* **280**:19146–19155.
- Zamze SE, Ferguson MA, Collins R, Dwek RA, and Rademacher TW (1988) Characterization of the cross-reacting determinant (CRD) of the glycosyl-phosphatidylinositol membrane anchor of *Trypanosoma brucei* variant surface glycoprotein. *Eur J Biochem* **176**:527–534.

---

**Address correspondence to:** Dr. Günter Müller, Sanofi-Aventis Pharma Germany GmbH, TD Metabolism, Industrial Park Höchst, Bldg. H821, 65926 Frankfurt am Main, Germany. E-mail: guenter.mueller@sanofi-aventis.com

---